^{13}C and ^{17}O NMR Binding Constant Studies of Uranyl Carbonate Complexes in Near-Neutral Aqueous Solution

Yucca Mountain Project Milestone Report 3351

Los Alamos
NATIONAL LABORATORY

DISCLAIMER

Portions of this document may be illegible in electronic image products. Images are produced from the best available original document.

^{13}C and ^{17}O NMR Binding Constant Studies of
Uranyl Carbonate Complexes in Near-Neutral
Aqueous Solution

Yucca Mountain Project Milestone Report 3351

David L. Clark
Thomas W. Newton
Phillip D. Palmer
Bill D. Zwick

MASTER

Los Alamos
NATIONAL LABORATORY

Los Alamos, New Mexico 87545

Table of Contents

List of Figures

List of Tables

Glossary of Acronyms

DOE	United States Department of Energy
EXAFS	Extended X-ray Absorption Fine Structure
NHE	Normal Hydrogen Electrode
NIR	Near Infra-Red
NMR	Nuclear Magnetic Resonance
OECD NEA	Organisation for Economic Co-operation and Development Nuclear Energy Agency
pH	$-\log(a_{H^+})$
p[H]	$-\log[H^+]$
PAS	Photoacoustic Spectroscopy
SCE	Saturated Calomel Electrode
SIT	Specific ion Interaction Theory
UV-VIS	Ultraviolet-Visible
XAS	X-ray Absorption Spectroscopy
YMP	Yucca Mountain Site Characterization Program

^{13}C and ^{17}O NMR Binding Constant Studies of Uranyl Carbonate Complexes in Near-neutral Aqueous Solution

Yucca Mountain Project
Milestone Report 3351

by

David L. Clark*, Thomas W. Newton, Phillip D. Palmer, and Bill D. Zwick

Abstract

Valuable structural information, much of it unavailable by other methods, can be obtained about complexes in solution through NMR spectroscopy. From chemical shift and intensity measurements of the complexed species, NMR can serve as a *species-specific* structural probe for molecules in solution and can be used to validate thermodynamic constants used in geochemical modeling. Fourier-transform nuclear magnetic resonance (FT-NMR) spectroscopy has been employed to study the speciation of uranium(VI) ions in aqueous carbonate solutions as a function of pH, ionic strength, carbonate concentration, uranium concentration, and temperature. Carbon-13 and Oxygen-17 NMR spectroscopy were used to monitor the fractions, and hence thermodynamic binding constants of two different uranyl species $UO_2(CO_3)_3^{4-}$ and $(UO_2)_3(CO_3)_6^{6-}$ in aqueous solution. Synthetic buffer solutions were prepared under the ionic strength conditions used in the NMR studies in order to obtain an accurate measure of the hydrogen ion concentration, and a discussion of pH = $-\log(a_{H^+})$ versus p[H] = $-\log[H^+]$ is provided. It is shown that for quantitative studies, the quantity p[H] needs to be used. Fourteen uranium(VI) binding constants recommended by the OECD NEA literature review were corrected to the ionic strengths employed in the NMR study using specific ion interaction theory (SIT), and the predicted species distributions were compared with the actual species observed by multinuclear NMR. The agreement between observed and predicted stability fields is excellent. This NMR study establishes the utility of multinuclear NMR as a *species-specific* tool for the study of the actinide carbonate complexation constants, and serves as a means for validating the recommendations provided by the OECD NEA. This study also demonstrates that multinuclear NMR studies can be used to unequivocally identify and measure the thermodynamic binding constants of transuranic actinide carbonate and hydroxide complexes which are not well understood.

1

1.0 Introduction.

Carbonate and bicarbonate are common anions found in significant concentrations in many natural waters, and represent exceptionally strong complexation agents for actinide ions.[1-4] Therefore, carbonate complexes of the actinide ions may play an important role in migration from a nuclear waste repository or in accidental site contamination.[5,6] The potential for aquatic transport of actinides by carbonate complexation is reflected in the formation of uranyl carbonate containing minerals such as Rutherfordine, $UO_2(CO_3)$,[7] and Andersonite, $Na_2Ca[UO_2(CO_3)]\cdot 6H_2O$.[8]

A detailed understanding of the chemical equilibria and the formation constants that link the various actinide carbonate species is needed so that thermodynamic modeling can accurately predict radionuclide speciation and solubility. A common method for measurement and refinement of equilibrium constants is potentiometric titration, and curve-fitting the data to a set of thermodynamic constants.[9] The computer codes used in the fitting are so prevalent and easy to use that in some cases, so many species have been used to fit the observed data, that the resulting parameters are meaningless. The problems of low-quality data and putative species makes it necessary from a quality assurance standpoint to have alternate methods available with which to test the validity of the available data, and to determine new or unknown binding constants for transuranium elements. Along these lines, the OECD Nuclear Energy Agency (NEA) has initiated a series of detailed expert reviews of the chemical thermodynamics of key elements in nuclear technology and waste management, and the first volume on the chemical thermodynamics of uranium has been published.[6] The objective of the uranium review was to present an assessment of the sources of published thermodynamic data in order to decide on the most reliable values for recommended use. The NEA reviewers point out that while it is possible to obtain a unique chemical model in terms of the empirical formula, additional chemical information is still needed to determine the molecular complexity of the system. Valuable structural information, much of it unavailable by other methods, can be obtained about complexes in solution through Nuclear

2

Magnetic Resonance (NMR) spectroscopy. From chemical shift measurements of the complexed species, NMR can serve as a *species-specific* structural probe for molecules in solution. For a binding system in the slow chemical exchange limit, the NMR experiment yields the area of the resonance peaks of the nucleus under observation in different chemical environments. From the integrated intensities the ratio of the concentrations of the species is obtained, and the binding constant calculated with the additional knowledge of the concentrations. Based on this discussion, it is somewhat surprising that relatively few NMR studies of actinyl carbonate systems have appeared. We initiated a program to evaluate the applicability of multinuclear NMR spectroscopy as a *species-specific* probe to track relative concentrations, and hence species distributions of actinide carbonate complexes as a function of -log[H$^+$]. The distribution of species observed by multinuclear NMR can be compared with predictions from other data, recorded at lower concentrations, and may serve as a method for database validation. This is an important exercise because thermodynamic information is needed to resolve performance and design issues related to a potential high level nuclear waste repository.

1.1 The Uranyl Carbonate System. Actinide carbonate systems are usually quite complicated in that they consist of several different complex ions in rapid equilibria with one another and with uncomplexed or hydrolyzed species. The uranium carbonate system is by far the most extensively studied of all actinide carbonate systems and is therefore the most well-suited system for testing the applicability of multinuclear NMR speciation studies.[10-27] From all the available literature, the composition and molecular structure of the limiting complex of formula $AnO_2(CO_3)_3^{4-}$ is well established for the early actinides U, Np, Pu, and Am.[8,16,20,28-35] For species of general formula $AnO_2(CO_3)_2^{2-}$, a trimeric species of composition $[AnO_2(CO_3)_2]_3^{6-}$ has been reported for An = U,[16] and is believed to be important for Np and Pu.[36] This trimer is strongly stabilized in solutions of high ionic strength, and is thought to be responsible for the very high solubility of $AnO_2CO_3(s)$ in carbonate solutions, and thus may have important implications for

aquatic transport of actinyl ions through carbonate complexation. The molecular structure of the monomeric $UO_2(CO_3)_3^{4-}$, based on single crystal X-ray diffraction is shown schematically in **1** below,[8] and the proposed structure of the trimer, $(UO_2)_3(CO_3)_6^{6-}$, which is based on the solid-state structure of Rutherfordine is shown in **2**, below.[16]

1   **2**
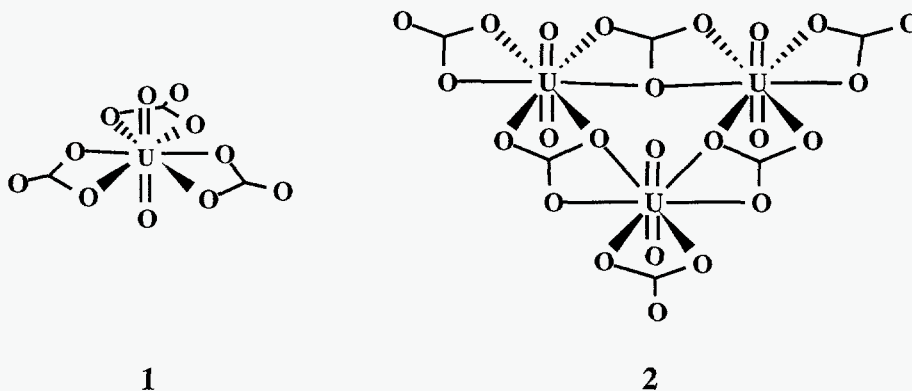
Ciavatta *et. al.* was the first to identify the presence of $(UO_2)_3(CO_3)_6^{6-}$ through potentiometric (emf) titration studies.[16] These workers also reported ^{13}C NMR data for a sample at pH 5.7 at both 25 and 0 °C.[24] Thier NMR data showed two ^{13}C NMR resonances consistent with the structure proposed in **2**. Several years later, Glaser *et. al.* reported an ^{17}O NMR spectrum of a sample believed to have the same composition as that reported by Ciavatta, and these workers observed five ^{17}O NMR signals between δ 1130 - 1095 ppm in the expected 2:2:2:1:1 ratio.[37] Since there are five different oxygen atom environments in a 6:6:6:3:3 ratio in the proposed trimeric structure, it was argued that this ^{17}O NMR spectrum confirmed the solution structure of $(UO_2)_3(CO_3)_6^{6-}$ as that shown in 2. However, upon further consideration of this data, we note that all five ^{17}O resonances reported for $(UO_2)_3(CO_3)_6^{6-}$ appear in the uranyl (O=U=O) chemical shift region of the ^{17}O NMR spectrum. Since carbonate oxygen signals should appear in a region of the spectrum near 200 ppm, the observed signals cannot be due to the five types of oxygen present in the trimer, but are more consistent with five different uranyl oxygen environments. Either there were multiple uranyl-containing species present in Glaser's solution, or the structure of the trimer is extremely more complex than originally proposed. Due to the discrepancies noted

4

above, the uranyl triscarbonate system is in need of a detailed multinuclear NMR titration study to help resolve the discrepancies, and assess the applicability of NMR for the general study of transactinide carbonate systems.

2.0 Results and Discussion.

2.1 General Synthetic Considerations Regarding Isotopic Enrichment. Since carbon and oxygen atoms appear as the major atomic constituent of actinyl carbonate complexes, the carbon and oxygen NMR spectra of carbonate complexes should contain much useful information regarding speciation in aqueous solution. However, the ^{12}C and ^{16}O nuclei are not magnetically-active since they have no net nuclear spin (I = 0). In contrast, the ^{13}C and ^{17}O nuclei, like the ^1H nucleus, do have a net nuclear spin (I = 1/2 and 5/2 respectively) and will give rise to an NMR signal. However, the natural abundance of ^{13}C and ^{17}O is only 1.1 and 0.037% respectively.[38] In addition, the sensitivity of these nuclei is only about 1.6 and 2.9% that of ^1H, so the overall sensitivity of ^{13}C compared with ^1H is about 1/5700, and ^{17}O compared to ^1H is about 1/9300.[38] Finally, the carbonate ligand has no attached protons so there is no nuclear Overhauser enhancement (NOE) of the ^{13}C or ^{17}O NMR signals for this ligand. Therefore, it is advantageous to isotopically-enrich the ligand in the spin-active ^{13}C or ^{17}O nucleus for NMR observation. The ^{17}O NMR nucleus is also notoriously difficult to observe by NMR since it is a spin 5/2 nucleus with an appreciable quadrupole moment leading to rapid nuclear quadrupole relaxation.[39,40] This rapid relaxation is advantageous since it allows rapid RF pulsing in the FT NMR method. However, it also leads to broad NMR resonances, hence poor spectral resolution and signal to noise ratios. Furthermore, this rapid transverse relaxation necessitates the use of short delay times between the end of each RF pulse and the beginning of data acquisition, often resulting in incomplete spectrometer recovery and consequently baseline distortion due to pulse breakthrough in the transformed spectra. Nevertheless, the experience gained in the few investigations that have appeared in the literature shows that the synthetic efforts to enrich the

samples are justified by the significance of the information obtained.[39,40] Therefore, we sought general synthetic methods for enrichment of both ^{13}C and [17]O isotopes in the uranyl carbonate system.

2.1.1 Synthesis of [13]C Labeled Compounds.

[13]C labeling was achieved through the use of 99.9% ^{13}C-enriched Na_2CO_3. Single crystals of triply recrystallized $UO_2(ClO_4)_2 \cdot 6H_2O$ were dissolved in D_2O. Three equivalents of $Na_2{}^{13}CO_3$ were also dissolved in D_2O and added dropwise with stirring to the uranyl solution to form the triscarbonate complex according to the stoichiometry indicated in equation 1 (where * represents 99.9% [13]C). $NaClO_4 \cdot H_2O$ was then added to the resulting uranyl carbonate solution to adjust the ionic strength to between 4.0 - 2.5 moles/kg. $1M$ $HClO_4$ was used to adjust the pH of the solution to get 5 - 17 samples with pH values ranging from $5.7 \leq pH \leq 9.0$. All samples were flame-sealed in standard high precision 5mm glass NMR tubes. Those samples prepared at pH values below 6.5 were sealed in tubes flushed with CO_2 in order to stabilize the observed pH.

$$UO_2(ClO_4)_2 + 3\,Na_2{}^*CO_3 \quad \xrightarrow{\ D_2O\ } \quad UO_2({}^*CO_3)_3{}^{4-} + 6\,Na^+ + 2\,ClO_4{}^- \qquad (1)$$

2.1.2 Synthesis of [17]O Labeled Compounds.

It is well-known that photolysis of uranyl solutions in [17]O-enriched water will efficiently incorporate the [17]O nucleus into the uranyl oxygen sites of uranyl containing compounds.[41,42] While this technique works extremely well for the uranyl ion, it is well-known that oxygen isotope exchange in $NpO_2{}^{n+}$, and presumably other transuranic actinyl ions is notoriously slow.[43] Therefore, we sought a general synthetic approach that would work for all the actinyl ions, and could be employed in future studies of the transuranic actinyl systems. Since the electrochemistry of aqueous solutions of the actinide ions under acidic conditions is well-established and commonly used to prepared oxidation-state pure actinide ions,[44]

we examined the utility of electrochemical synthesis for ^{17}O isotopic enrichment of early actinyl ions of U, Np, Pu, and Am.

Single crystals of triply-recrystallized $UO_2(ClO_4)_2 \cdot 6H_2O$ were dissolved in a mixture of $D_2O:H_2{}^{17}O$ to make a 0.4 M solution of the $UO_2{}^{2+}$ ion that was 10% enriched in the ^{17}O isotope. The uranyl solution was electrolytically reduced to the aquo U^{4+} ion in 1.5M $HClO_4$ in the presence of ^{17}O-enriched water using a conventional 3-electrode system as outlined in equation 2. The reduction of the metal ion from U(VI) to U(IV) is accompanied by the complete removal of the oxo ligands.[45] The resulting U(IV) ion is coordinated only by water molecules in the coordination sphere in the form of $U(*OH_2)_n{}^{4+}$, where * represents 10% ^{17}O-enriched oxygen. The reduction is conveniently monitored by UV-VIS spectroscopy by following the disappearance of the 414 nm absorption band of U(VI) and appearance of the 648 nm absorption band of U(IV). The U(IV) solution was subsequently electrochemically re-oxidized to the $UO_2{}^{2+}$ ion resulting in a $UO_2{}^{2+}$ solution that was 10% enriched in ^{17}O as indicated in equation 3. Addition of carbonate-free NaOH to the ^{17}O-enriched uranyl solution results in precipitation of a bright-yellow hydroxide between $4.5 \leq pH \leq 7$ as indicated in equation 4. Precipitation provides a solid material that can be isolated free from acid by centrifugation and multiple washings with distilled water. Care must be exercised to keep the pH below 7. When precipitation occurred at pH values greater than 7, the resulting solid would not redisolve in bicarbonate solution. In another step, ^{17}O-enriched $HCO_3{}^-$ was prepared by placing a 0.6M NaOH solution under 5 atmospheres of CO_2 in a PARR bomb reactor. The solution was allowed to equilibrate for 12 hours with stirring and resulted in a weakly acidic ^{17}O-enriched $(5 \leq pH \leq 6)$ $HCO_3{}^-$ solution as indicated in equation 5. The ^{17}O-enriched uranyl hydroxide precipitate from equation 4 was dissolved in the freshly-prepared ^{17}O-enriched $HCO_3{}^-$ to make a solution of $U^{17}O_2 (C^{17}O_3)_3{}^{4-}$ that was ^{17}O-enriched in all oxygen sites as indicated in equation 6. $NaClO_4 \cdot H_2O$ was added to make the ionic strength of solution 3.3 mol/kg. 1M $HClO_4$ and solid Na_2CO_3 were used to adjust the pH and obtain samples in the pH

range from $6.0 \leq pH \leq 9.7$. Samples were flame-sealed in precision 5mm glass NMR tubes and pH values near a pH of 6 were stabilized by using CO_2 flushed NMR tubes.

$$U^{VI}O_2(OH_2)_n^{2+} \xrightarrow[+\,2e^-]{H_2^*O} U^{IV}(^*OH_2)_n^{4+} \tag{2}$$

$$U^{IV}(^*OH_2)_n^{4+} \xrightarrow[-\,e^-]{H_2^*O} U^{V^*}O_2(^*OH_2)_n^+ \underset{+\,e^-}{\overset{-\,e^-}{\rightleftharpoons}} U^{VI^*}O_2(^*OH_2)_n^{2+} \tag{3}$$

$$U^{VI^*}O_2(^*OH_2)_n^{2+} \xrightarrow[OH^-]{4.5 \leq pH \leq 7} U^{VI^*}O_2(^*OH)_2 \tag{4}$$

$$H_2^*O \xrightarrow{NaOH} H^*O^- \xrightarrow[5\,atm]{CO_2} HC^*O_3^- \tag{5}$$

$$U^{VI^*}O_2(^*OH)_2 + 3\,HC^*O_3^- \longrightarrow U^{VI^*}O_2(C^*O_3)_3^{4-} + 2\,H_2^*O + H^+ \tag{6}$$
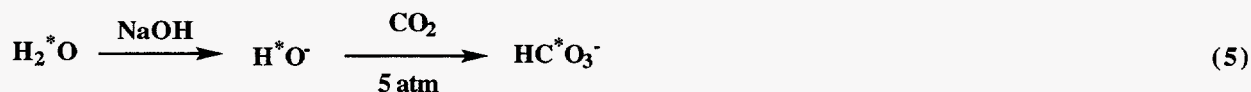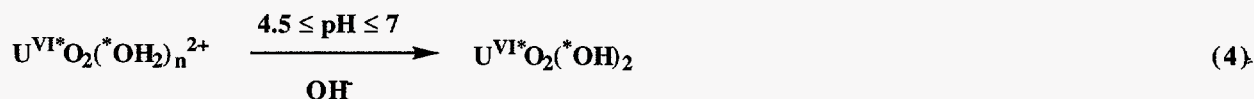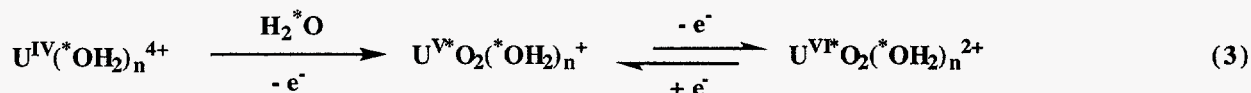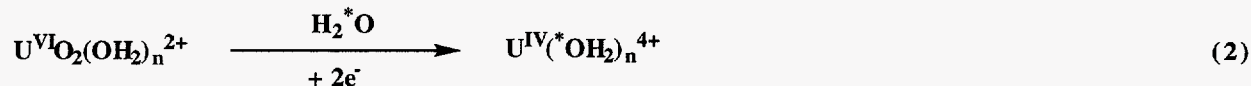
2.1.3 Synthesis of crystalline samples.

In addition to the synthesis of isotopically-enriched complexes for study by multinuclear NMR spectroscopy, we also wanted to prepare analytically-pure crystalline samples for characterization by x-ray diffraction techniques. Our study of solution NMR samples revealed the conditions under which we could reproducibly prepare stable solutions. This understanding of the solution behavior allowed for the preparation of samples that contained nearly pure monomeric $UO_2(CO_3)_3^{4-}$ or trimeric $(UO_2)_3(CO_3)_6^{6-}$ anions. We then added varying amounts of counter cations to these solutions, followed by slow cooling to 5 °C in attempts to isolate crystalline samples suitable for X-ray diffraction studies. The following cations produced either amorphous or microcrystalline precipitates, or clear solutions: Na^+, K^+, $(CH_3)_4N^+$, $(CH_3CH_2)_4N^+$, $(CH_3CH_2CH_2)_4N^+$, and $(C_6H_5)_3(CH_3)N^+$. We also examined the use of cryptands such as Kryptofix 222 (4,7,13,16,21,24-hexaoxa-1,10- diazabicyclo-[8.8.8]hexacosane), Kryptofix 211 (4,7,13,18-tetraoxa-1,10-diazabicyclo[8.5.5]eicosane) and

crown ethers such as 18-crown-6 (1,4,7,10,13,16-hexaoxacyclooctadecane) in the presence of Na^+ or K^+ ions. None of these attempts provided crystalline samples. However, we did discover that the guanidinium cation $C(NH_2)_3^+$ produced nice single crystals of compounds of empirical formula $[UO_2(CO_3)_3][C(NH_2)_3]_4$ and $[UO_2(CO_3)_2][C(NH_2)_3]_2$ based on combustion elemental analysis. Crystalline samples of trimeric $[(UO_2)_3(CO_3)_6][C(NH_2)_3]_6$ were prepared as outlined in equation 7. Monomeric $[UO_2(CO_3)_3][C(NH_2)_3]_4$ crystals were suitable for single crystal x-ray diffraction analysis, while crystals of trimeric $[UO_2(CO_3)_2]_3[C(NH_2)_3]_6$ were too small and thin for normal diffraction techniques. However, it is anticipated that x-ray diffraction using a rotating anode may prove fruitful in determining the solid-state molecular structure of this fundamentally important compound.

$$3[UO_2(CO_3)_3][C(NH_2)_3]_4 + 6H^+ \longrightarrow [(UO_2)_3(CO_3)_6][C(NH_2)_3]_6 + 3H_2O + 3CO_2 \quad (7)$$
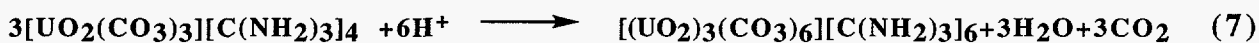
2.2 Multinuclear NMR Measurements.

2.2.1 ^{13}C NMR Measurements. We examined the uranyl carbonate system using ^{13}C NMR spectroscopy of 99.9% ^{13}C-enriched $UO_2(^{13}CO_3)_3^{4-}$ at 0.2 and 0.05 M uranyl concentrations corresponding to ionic strengths of 4.0 and 2.5 moles/kg. Original solutions were prepared with a carbonate-to-metal ratio of 3:1 which should favor the monomeric $UO_2(CO_3)_3^{4-}$ complex. Careful addition of $HClO_4$ protonates the carbonate ligand allowing for a decrease in the carbonate:uranyl ratio to 2:1 in a slow and controlled fashion as outlined in equation 8.[23]

$$3\ UO_2(CO_3)_3^{4-} + 6H^+ \rightleftharpoons (UO_2)_3(CO_3)_6^{6-} + 3\ HCO_3^- \quad (8)$$
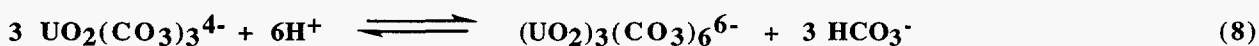
NMR samples were flame-sealed in precision glass NMR tubes and allowed to come to equilibrium for approximately 48 hours. The ^{13}C NMR spectra were recorded at 23 °C and a representative series of spectra are shown in Figure 1. Solution conditions are given in the figure

caption. At pH values above 8.0, a single ^{13}C NMR resonance is observed at δ 165.2 ppm (Figure 1) and can be assigned to the terminal carbonate ligand in monomeric $UO_2(CO_3)_3^{4-}$. At pH 7.5 a new ^{13}C resonance {presumably due to trimeric $(UO_2)_3(CO_3)_6^{6-}$} appears at δ 166.2 ppm. It is apparent at pH 7.5 that the original resonance at δ 165.2 ppm begins to show some line-broadening, and at pH 7.0, a well-defined shoulder at δ 164.9 ppm can be seen on the right hand side of the original NMR resonance line centered at δ 165.2 ppm. As the titration continues, the original monomer resonance at δ 165.2 disappears and the two new resonances of a new species grow in as shown in Figure 1. It is noteworthy that one of the NMR signals observed at pH 6.0 is relatively sharp, while the other is broad, suggesting that chemical exchange is occurring during the timescale of the NMR experiment. When the ^{13}C NMR spectra of the uranyl carbonate system is recorded at 0 °C, chemical exchange is slowed and the line-width of the terminal carbonate resonances in both monomer and the new (presumably trimeric) species sharpen. A stacked plot of this same sample recorded at 0 °C is shown in Figure 2. From Figure 2 it can be seen that at 0 °C, the resonance at δ 164.9 has sharpened considerably, and the monomer resonance at δ 165.2 ppm has also sharpened due to the freezing out of chemical exchange.

The monomeric $UO_2(CO_3)_3^{4-}$ (1) has only one type of carbonate ligand environment, and thus gives rise to a single ^{13}C NMR resonance (δ 165.2 ppm) as seen in Figures 1 and 2 at pH 8.0. The proposed trimeric structure for $(UO_2)_3(CO_3)_6^{6-}$ (2) has two, equally populated carbonate ligand environments and should give rise to two, equal intensity resonances as seen in Figures 1 and 2 at pH 6.0. The observed ^{13}C NMR data is consistent with this structure proposed by Ciavatta et. al.[23] The chemical shift difference between the two carbonate signals indicates that the two carbonate carbon environments are very different. Since the monomer (1) has only terminal carbonate ligand which is observed at δ 165.2 ppm, this establishes the chemical shift region for the terminal carbonate ligands of this system. For the trimer (2) we assign the high field resonance at δ 164.9 ppm to the terminal carbonate ligand, and the lower field resonance at δ = 166.2 ppm to
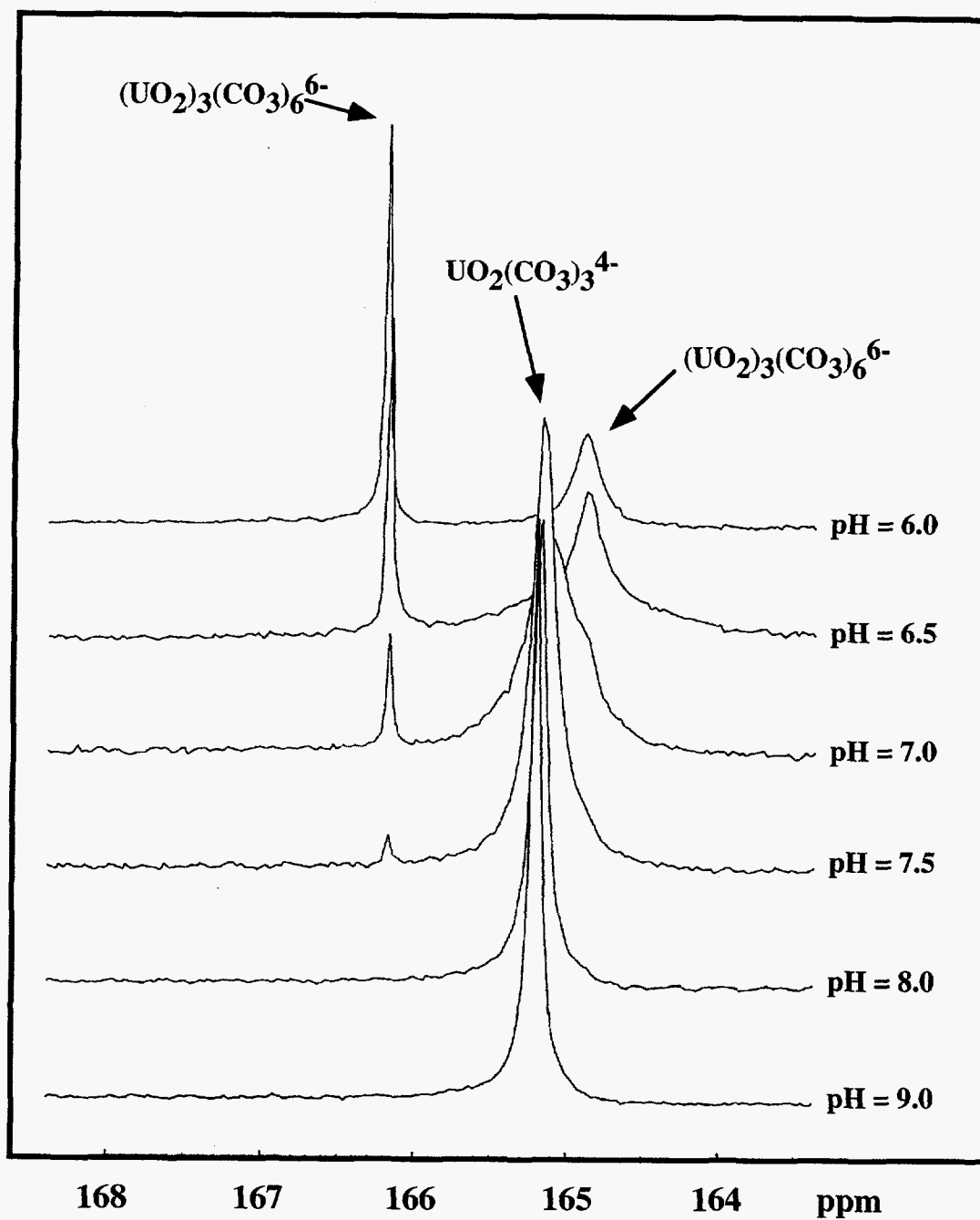
Figure 1. 62.9 MHz ^{13}C NMR spectra of a 0.2 M ($I_m = 4.1m$) uranyl carbonate solution at 23 °C as a function of pH. Carbon resonances corresponding to the carbonate ligand in $UO_2(CO_3)_3^{4-}$ and $(UO_2)_3(CO_3)_6^{6-}$ are indicated.
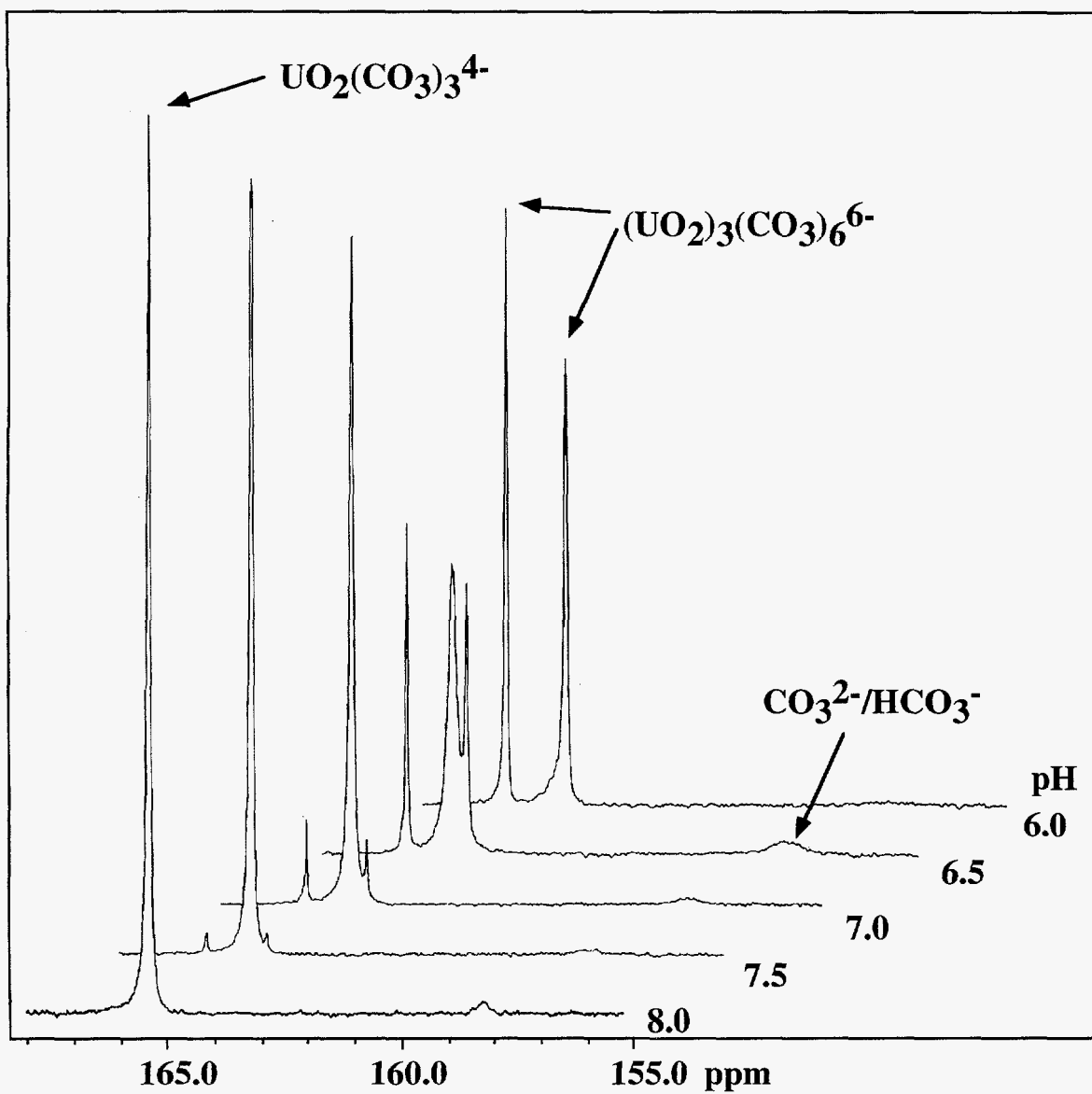
Figure 2. 62.9 MHz ^{13}C NMR spectra of a 0.2 M (I_m = 4.1m) uranyl carbonate solution at 0 °C as a function of pH. Carbon resonances corresponding to the carbonate ligand in $UO_2(CO_3)_3^{4-}$ and $(UO_2)_3(CO_3)_6^{6-}$ are indicated.

the bridging carbonate ligand. Figure 3 shows a ^{13}C NMR spectrum for a sample of nearly pure $(UO_2)_3(CO_3)_6^{6-}$ at pH 6.0 recorded at 0 and 23 °C. The NMR resonance lines appear in a 1:1 bridge:terminal ratio. Warming the sample results in a substantial line-broadening of the high field signal as shown in Figure 3. This is further indication that the resonance at δ 166 is due to a terminal ligand since carbonate ligand exchange is expected to be more facile for a terminal than a bridging ligand.

When the ^{13}C NMR spectra of the uranyl carbonate system is recorded at 0 °C, chemical exchange is slowed and the line-width of the terminal carbonate resonances in both monomer and trimer sharpen (Figure 2). Commensurate with the slowed exchange process, we can now observe free carbonate in the body of solution. It is the exchange between free carbonate in the body of solution and the terminal carbonate ligands in the uranyl carbonate complexes that causes the line-broadening in the terminal carbonate resonance. In addition, at pH values near 6.5 and lower, one observes free CO_2 dissolved in the solution. These observations are shown in Figure 4 for a representative sample recorded at 0 °C and pH 6.5. The above set of experiments established the ^{13}C NMR behavior for the uranyl carbonate system. A second, more detailed experiment was performed for a 0.05 M uranyl sample with an ionic strength of 2.5 moles/kg. A ^{13}C NMR titration of this sample performed at 0 °C and covering seventeen pH steps was examined for analysis of thermodynamic data, and a portion of this NMR titration is shown in Figure 5.

2.2.2 ^{17}O **NMR Measurements**. Once the conditions that favored monomer and trimer formation were well established by ^{13}C NMR, we sought to examine the equilibrium in even more detail using ^{17}O NMR spectroscopy. The integrated intensities of ^{17}O NMR resonances are generally only a qualitative measure of relative numbers of oxygen nuclei since relaxation rates for nonequivalent nuclei may vary, the RF pulse power decreases with increasing frequency from the transmitter, and audio frequency filtering decreases signal intensity in the same fashion. However, intensity data are quite reliable when resonances having similar line-widths and chemical shifts are
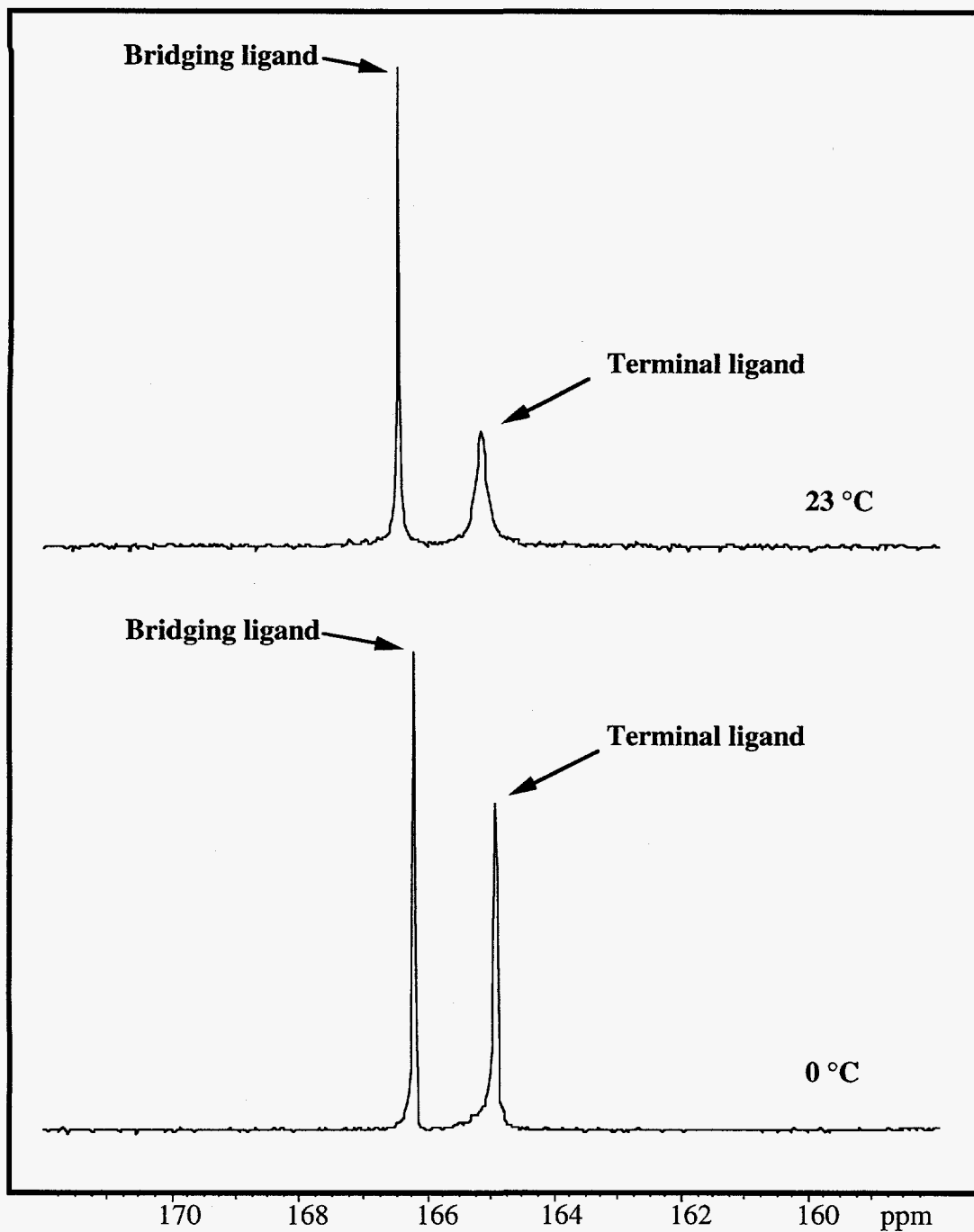
Figure 3. 62.9 MHz ^{13}C NMR spectra of a 0.2 M uranyl carbonate solution of nearly pure $(UO_2)_3(CO_3)_6^{6-}$ at pH 6.0 at 0 (bottom) and 23 °C (top). The increase in the line-broadening of the terminal carbonate resonance with increasing temperature is shown.
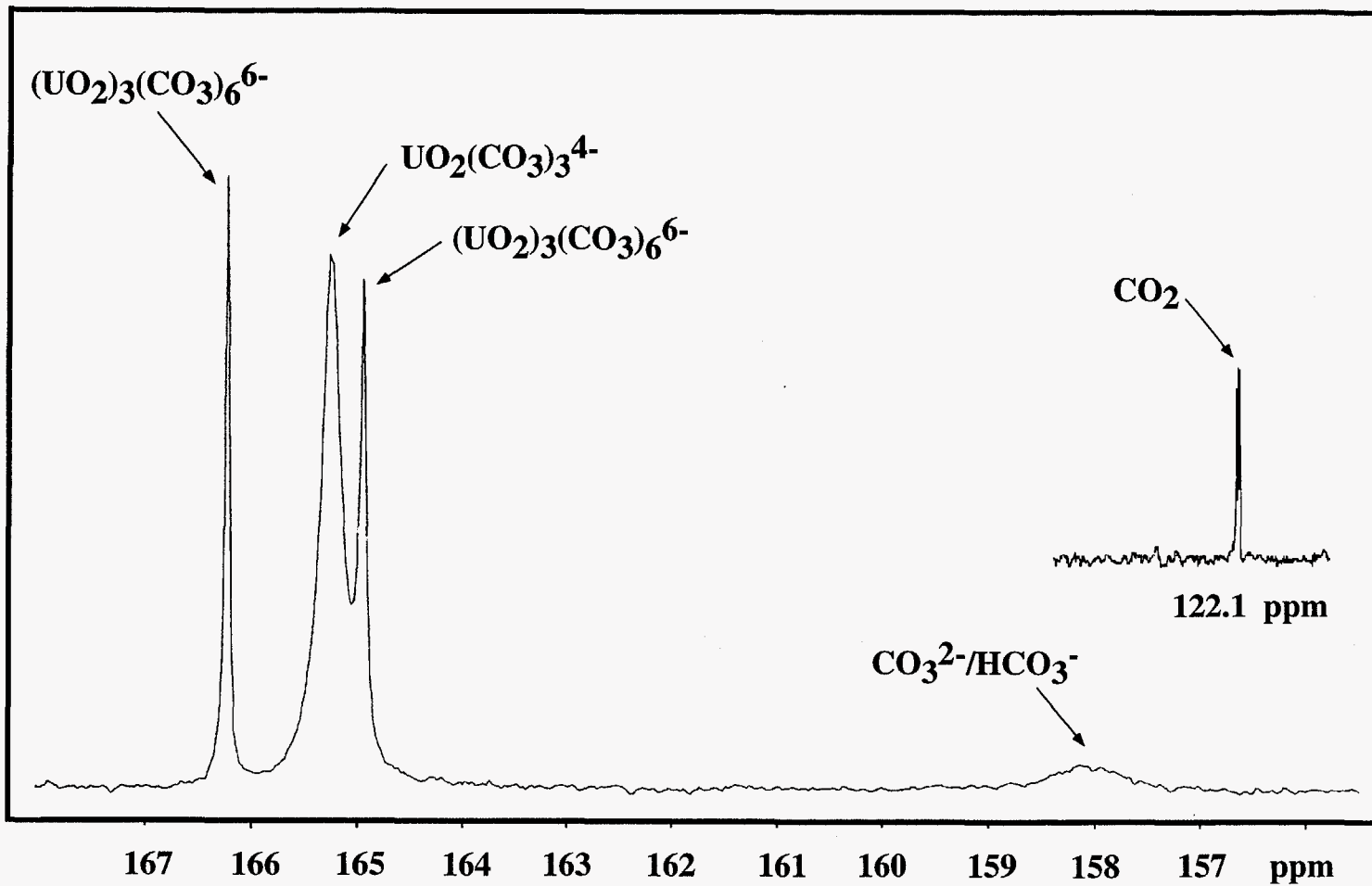
Figure 4. 62.9 MHz ^{13}C NMR spectra of a 0.2 M uranyl carbonate solution of nearly equal mixture of monomeric $UO_2(CO_3)_3^{4-}$ and trimeric $(UO_2)_3(CO_3)_6^{6-}$ at pH 6.5 at 0 °C.

15
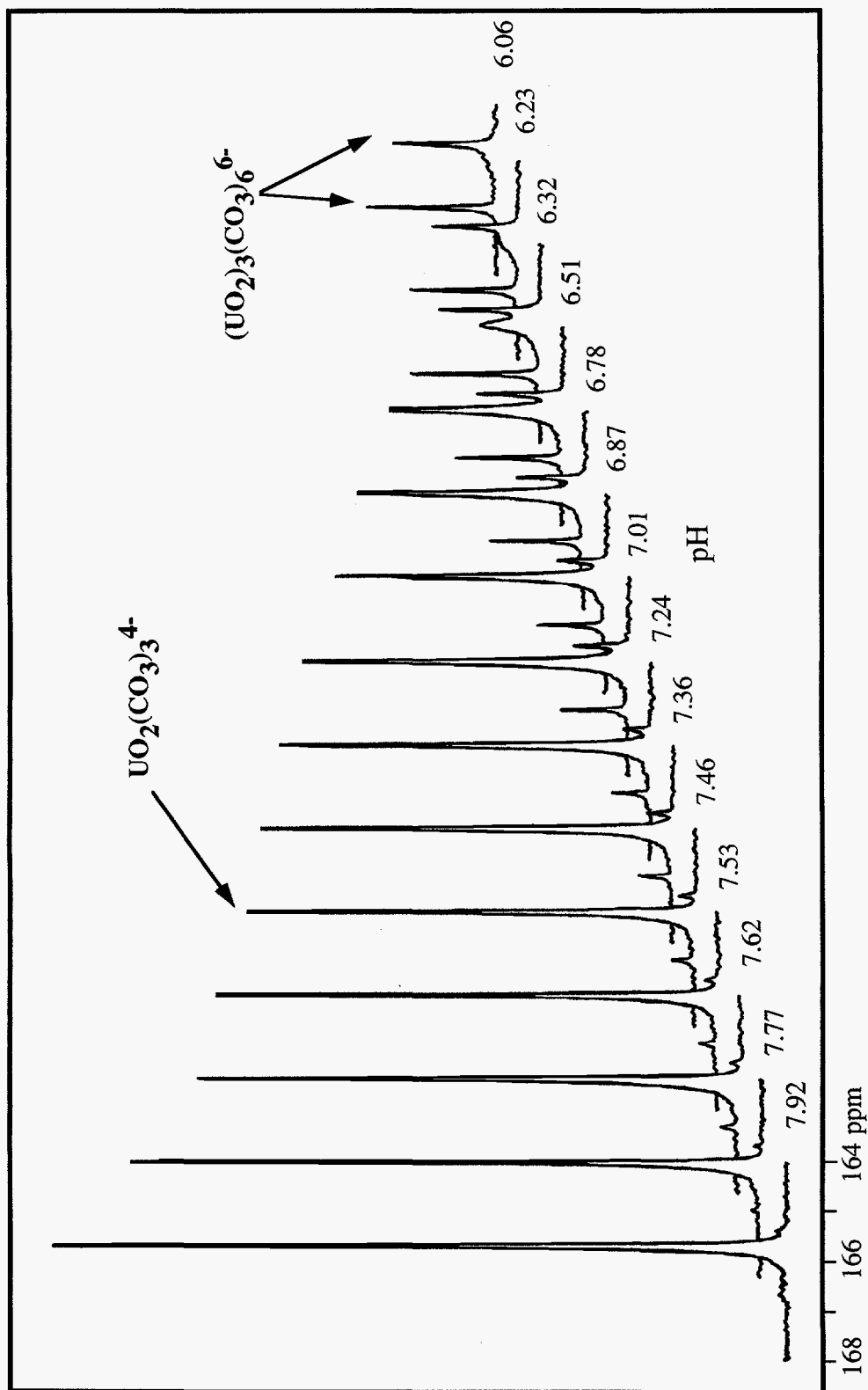
Figure 5. 62.9 MHz ^{13}C NMR spectra of a 0.05 M uranyl carbonate solution at 2.5 molal ionic strength as a function of p[H] at 0 °C.

16

compared as in this study.[39] Chemical shift data provide the most readily interpreted structural information.

Our first concern was to establish the chemical shift region for the uranyl and carbonate oxygen atoms in the ^{17}O NMR spectra of the individual components. ^{17}O-enriched samples of the uranyl and carbonate ions were prepared as outlined in equations 3 and 5 respectively. ^{17}O NMR spectra for the ^{17}O-enriched HCO_3^- ion recorded at pH 8.3 is shown in Figure 6. The observed chemical shift of δ 172 ppm compares favorably to the value of δ 192 ppm observed for the CO_3^{2-} ion in $0.1M$ KOH solution.[46] Since the chemical shift is a weighted average of CO_3^{2-} and HCO_3^- chemical shifts, its position will be very sensitive to pH. The broad linewidth of the HCO_3^- ion ($\Delta v_{1/2}$ = 200 Hz) is also a result of CO_3^{2-}/HCO_3^- chemical exchange. The observed chemical shift range of 170 - 200 ppm is in accord with the so-called "double-bond rule" in which chemical shifts are assumed to depend linearly on π bond order.[39,40] For example, a chemical shift of about 600 is observed for aldehydes and ketones (π bond order of 1), and this implies a chemical shift of about 200 for pure CO_3^{2-} (π bond order of 1/3). The observed shift of δ 192 for CO_3^{2-}, and 172 for HCO_3^- is in excellent agreement with this expectation. The ^{17}O NMR spectrum of the UO_2^{2+} aquo ion in $1M$ $HClO_4$ revealed a chemical shift of δ 1121 ppm for the uranyl bound oxygen atoms, and can be compared to δ 1119 ppm reported by Fukutomi.[47,48] The ^{17}O NMR spectrum of the uranyl ion in $1M$ $HClO_4$ is shown in Figure 7. These spectra of the free uranyl and bicarbonate/carbonate ions establish the chemical shift region that we can use as reference for future work on the carbonate complexation of actinyl ions.

^{17}O NMR analysis of a sample of ^{17}O-enriched monomeric $UO_2(CO_3)_4^{4-}$ (**1**) recorded at pH 9.7 revealed a uranyl oxygen in the expected chemical shift region at δ 1098 ppm, and two other oxygen resonances in the carbonate oxygen region at δ 225 and 185 ppm. This ^{17}O NMR spectrum is shown in Figure 8. An expanded view of the carbonate region of the spectrum is shown in the inset of Figure 8. The uranyl oxygen resonance at δ 1098 is relatively sharp as expected. Both resonances in the carbonate chemical shift region are very broad and indicative of
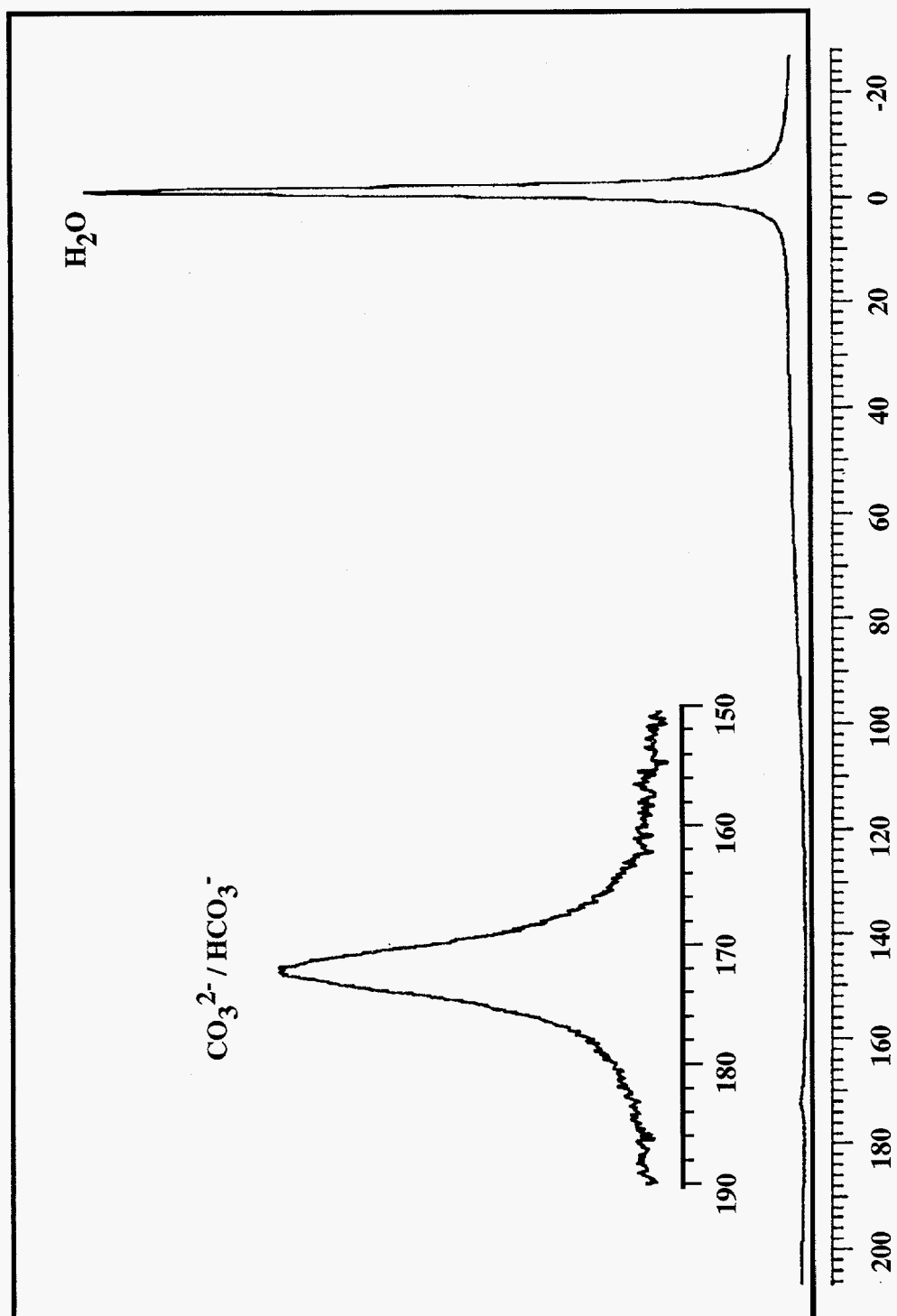
Figure 6. 40.7 MHz ^{17}O NMR spectrum of an ^{17}O-enriched CO_3^{2-}/HCO_3^- solution at pH 8.3 at 0 °C.
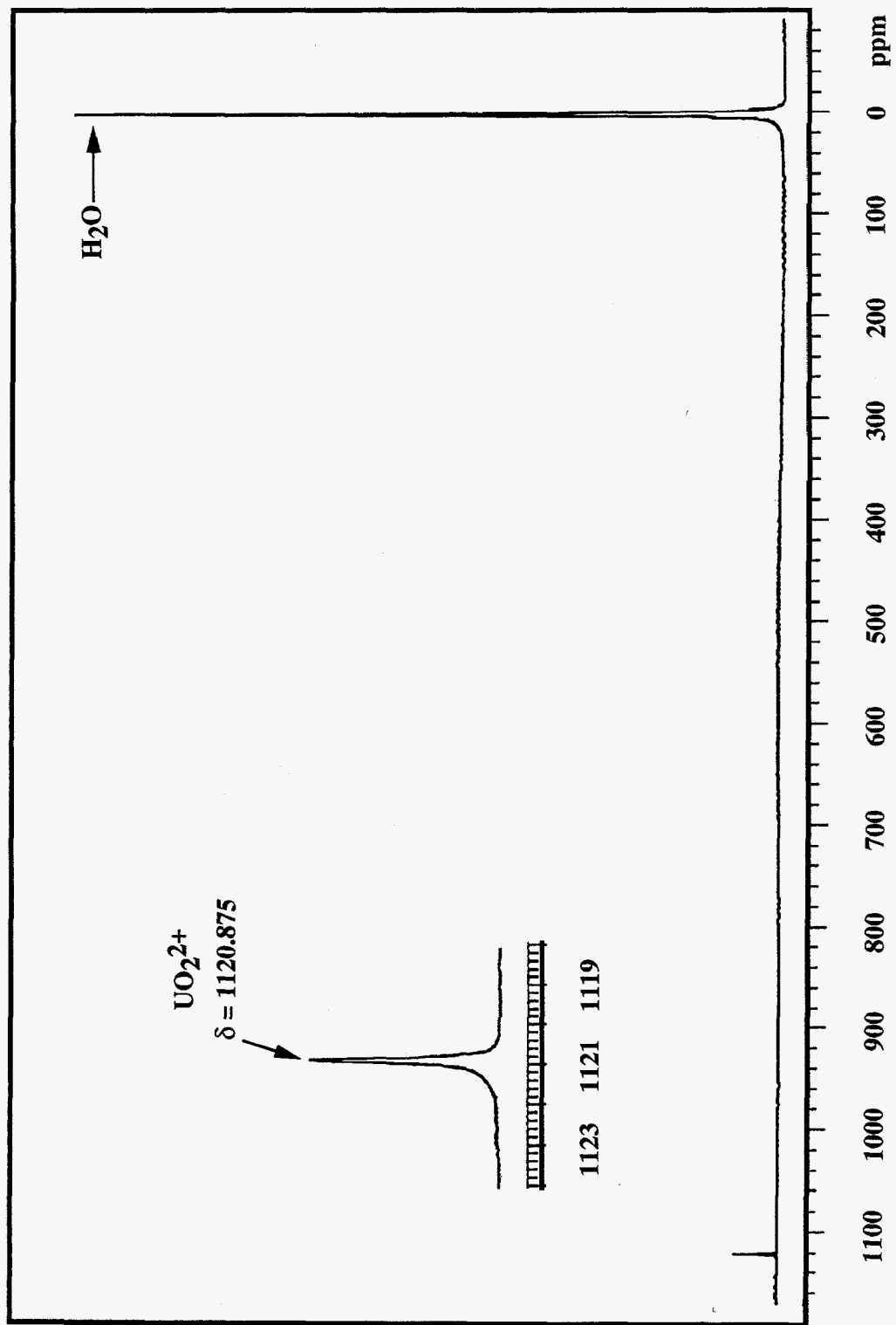
Figure 7. 40.7 MHz ^{17}O NMR spectrum of ^{17}O-enriched UO_2^{2+} in $1M$ $HClO_4$ at 17 °C.
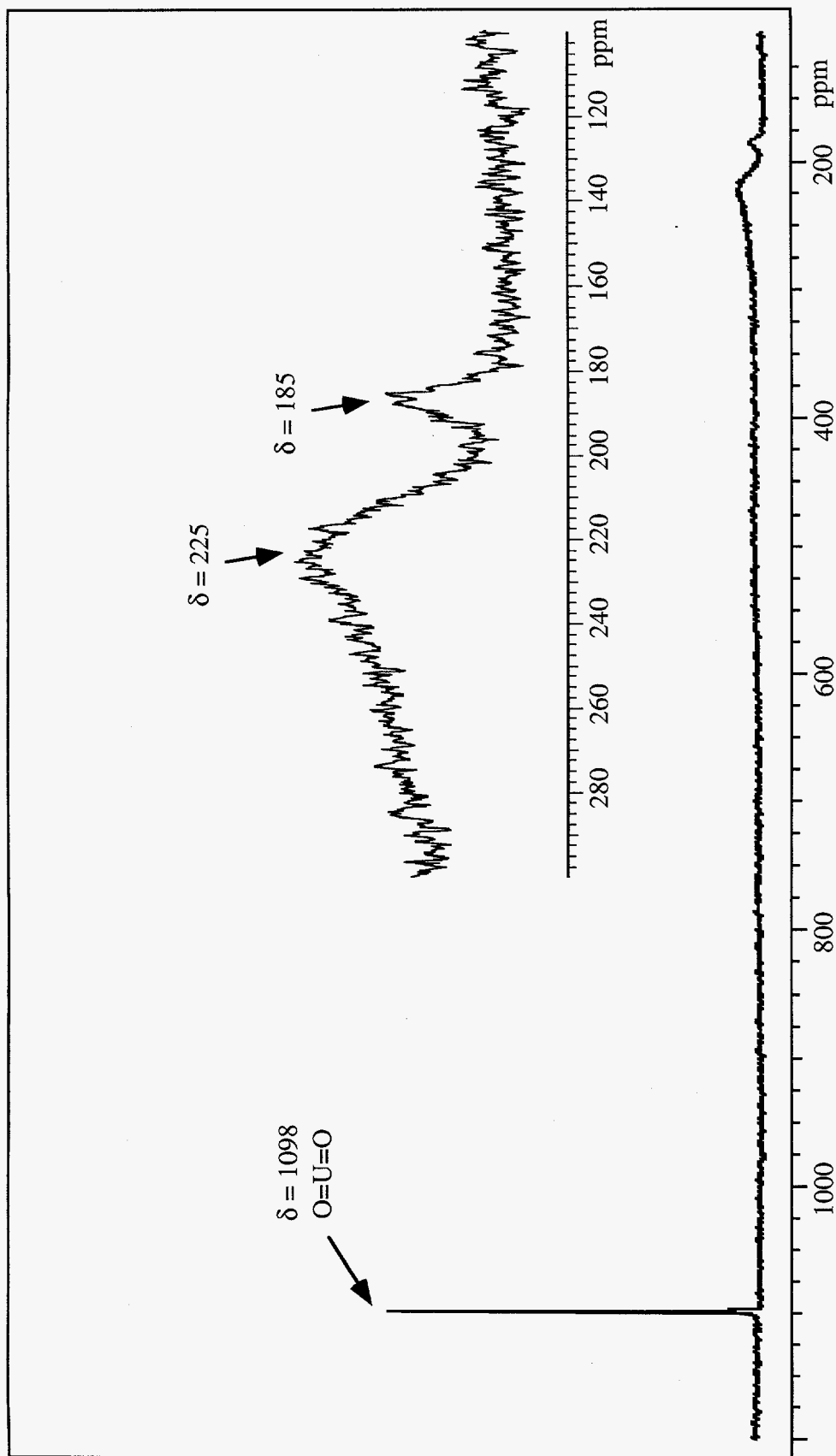
Figure 8. 33.9 MHz ^{17}O NMR spectrum of fully ^{17}O-enriched $UO_2(CO_3)_3^{4-}$ at pH 9.7 and 0 °C.

20

chemical exchange. The resonance at δ 185 ppm is consistent with free carbonate/bicarbonate ions in solution. The other resonance at δ 225 ppm is consistent with carbonate ligands in the coordination sphere of the uranyl ion. These spectra further establish the chemical shift regions in which we should expect to observe uranyl and carbonate oxygen atoms in the uranyl carbonate complexes.

The equilibrium in equation 8 was followed by ^{17}O NMR spectroscopy in approximately 0.25 pH unit increments between $6.0 \leq pH \leq 7.8$. The carbonate oxygen resonances seen at δ 185 and 225 at pH 9.7 (Figure 8) undergo coalescence upon a lowering of the pH below 9, and this is undoubtedly a result of an increase in the rate of carbonate ligand exchange upon lowering the pH. The uranyl oxygen resonances remain sharp since it is well-known that these oxygen atoms do not undergo appreciable oxygen atom exchange on the NMR timescale. Thus at the low field-strengths employed in this study, the carbonate oxygen resonances will be of little use due to exchange broadening. The uranyl oxygen region of the ^{17}O NMR spectra at 0 °C is extremely useful and is shown in Figure 9. At pH 7.87, there is a single uranyl-containing species at δ 1098 ppm. We have already established that this resonance is attributable to the uranyl oxygen atoms in monomeric $UO_2(CO_3)_3^{4-}$. As the NMR titration continues, a second uranyl oxygen resonance appears at δ 1105 ppm. The resonance due to $UO_2(CO_3)_3^{4-}$ decreases while the new resonance assigned to the equivalent uranyl oxygen atoms in $(UO_2)_3(CO_3)_6^{6-}$ increases, until, at pH 6.0, the trimer, **2**, is the dominant uranyl-containing species in solution. This data tracks well with our ^{13}C NMR experiment and reveals that there are only two observable uranyl species in solution under these experimental conditions.

2.2.3 Discussion of NMR data. The NMR data amassed thus far is consistent with only two observable species under the conditions employed in this study. Potentiometric titration and other data have been interpreted in terms of the reaction shown in equation 8, and Ciavatta has proposed the structure shown in **2** for the trimeric $(UO_2)_3(CO_3)_6^{6-}$ ion.[16,20,21] The
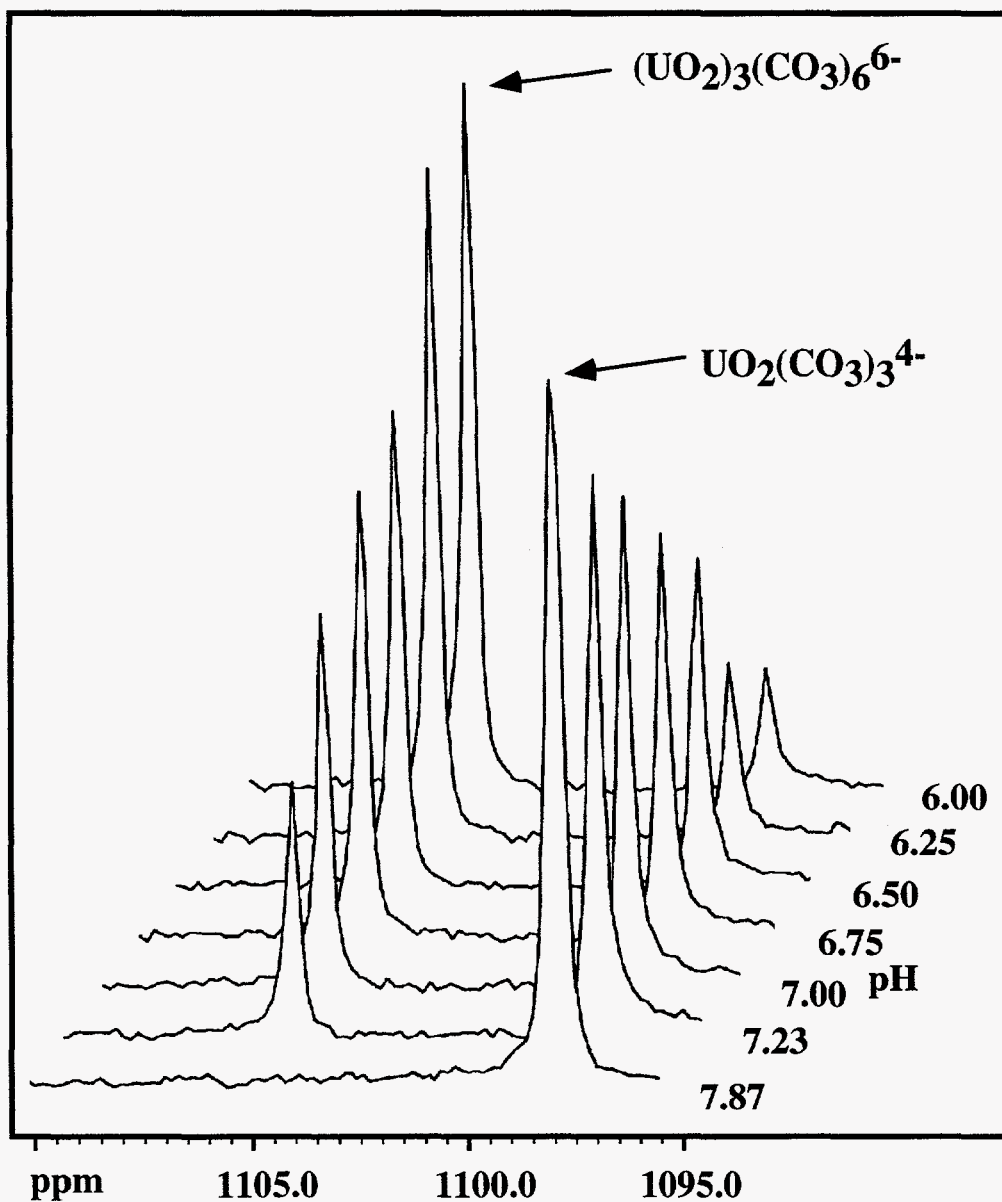
Figure 9. 33.9 MHz ^{17}O NMR spectra of a 0.2 M uranyl carbonate solution showing the fractions of monomeric $UO_2(CO_3)_3^{4-}$ and trimeric $(UO_2)_3(CO_3)_6^{6-}$ as a function of pH at 0 °C in the uranyl region of the ^{17}O NMR spectrum.

^{13}C and ^{17}O NMR data are consistent with the formation of this trimer. Unfortunately we are unable to observe the carbonate oxygen atoms due to chemical exchange at the low field strengths employed in this study. It is feasible that use of a much higher magnetic field strength will slow the chemical exchange and allow observation of all oxygen environments. Such an experiment was claimed, but it is clear from the data reported here that the previously reported spectrum shows only uranyl oxygen resonances.[37] We plan to perform this high field NMR experiment in the near future. In the absence of the penultimate NMR experiment, we must admit that the pattern of ^{13}C and ^{17}O NMR lines is equally consistent with formation of a dimer of formula $(UO_2)_2(CO_3)_4^{4-}$. For this reason we have made calculations to see whether an experimental U(VI) concentration dependence could be used to distinguish between a dimer and trimer. Log β_{36} can be assumed to be 0 and the value for log β_{24} determined (by trial and iteration) that gives the same equivalent fraction of $(UO_2)_2(CO_3)_4^{4-}$ as found previously for $(UO_2)_3(CO_3)_6^{6-}$. The input concentration of total $[UO_2^{2+}]$ was then reduced and the calculated fractions of $(UO_2)_2(CO_3)_4^{4-}$ and $(UO_2)_3(CO_3)_6^{6-}$ compared. For both p[H] values of 7.0 and 6.5, the two models differ significantly only at total uranium concentrations below about 0.01 M. It thus appears that an NMR experiment with $[UO_2^{2+}] = 0.01$ M, and long accumulation times might be able to distinguish between the two models. This experiment is planned for the future.

Further important insight regarding a possible dimer of formula $(UO_2)_2(CO_3)_4^{4-}$ comes from consideration and understanding of coordination chemistry. We believe that such considerations should not be overlooked in order to avoid the postulation of unjust species. The basic structural motif for monomeric $UO_2(CO_3)_3^{4-}$ contains the hexagonal bipyramidal coordination geometry as indicated in **1**.[8] A view looking down on the hexagonal plane in which uranyl oxygen atoms lie above and below the plane is shown in **3** below. It is a straightforward task to combine three hexagonal bipyramidal units to construct the proposed structure for a trimer of formula $(UO_2)_3(CO_3)_6^{6-}$ as shown looking down on the three-fold axis in **4**.[16] This unit gives rise to three terminal and three bridging carbonate ligands consistent with the observed NMR data.

If one were to construct a hypothetical dimeric unit while maintaining the terminal and bridging carbonate ligands based on the hexagonal bipyramidal coordination environment, a structure such as that shown in **5** results. This structure does not seem very reasonable due to the strain imposed on the bridging carbonate ligand.

3   **4**   **5**
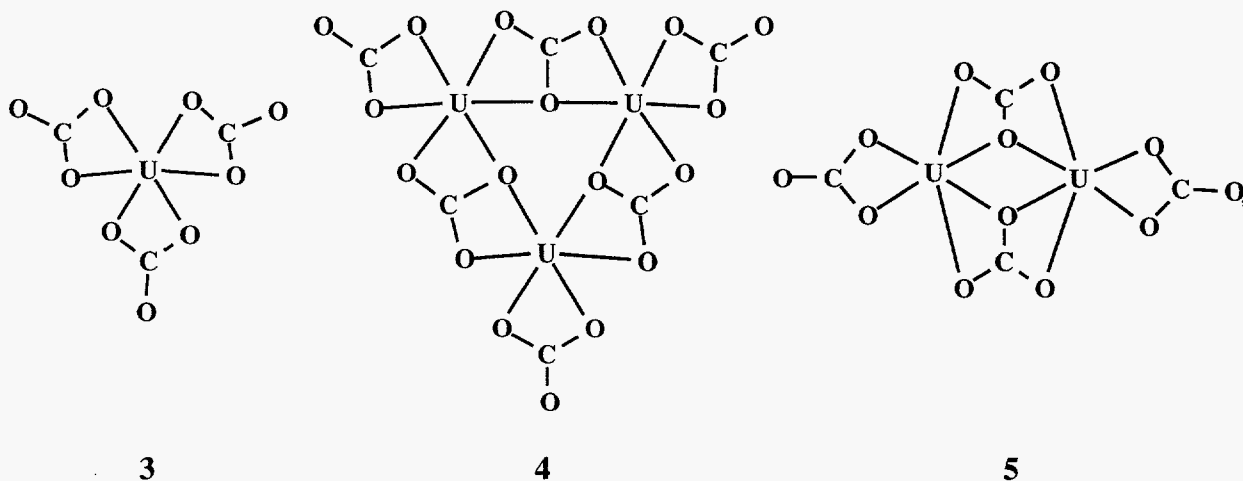
2.3   Analysis of Thermodynamic Data

2.3.1   General considerations. From the combination of ^{13}C and ^{17}O NMR integrations, one can extract the monomer and trimer concentrations directly for comparison with published thermodynamic data. The published data are generally measured at a variety of different conditions and need to be corrected to a standard thermodynamic state in order to make valid comparisons. Secondly, we need to determine the hydrogen ion concentration which is not the same as the pH. These data needs will be addressed in the subsequent sections.

2.3.2   Thermodynamic Binding Constants. The purpose of this study is to evaluate the applicability of multinuclear NMR spectroscopy as a *species-specific* probe to track relative concentrations, and hence species distributions of actinide carbonate complexes as a function of $-log[H^+]$. The distribution of species observed by multinuclear NMR can be compared

with predictions from other data, recorded at lower concentrations, and may serve as a method for database validation. This is an important exercise because thermodynamic information is needed to resolve performance and design issues related to a potential high level nuclear waste repository. In order to understand and model the total system, one needs to consider hydrolysis, carbonate complexation, and carbonate/bicarbonate equilibria. Log equilibrium quotients at zero ionic strength for hydrolyzed uranyl species were taken from the recently published OECD NEA review of uranium data.[6] The solubility product for $UO_2(OH)_2$ (s) was taken from the work of Baes and Mesmer.[49] The thermodynamic binding constants suggested by the NEA were used for the uranyl carbonate and hydroxy carbonate species.[6] The log equilibrium quotients used in our calculations are given in Table 1. Species other than those in these tables were not considered.

The equilibrium quotients from the literature need to be corrected so as to apply to the ionic strengths of the solutions considered in this study. The specific ion interaction theory (SIT) discussed in Appendix B of the NEA review was used.[6] The appropriate interaction coefficients are from Tables B.3 and B.4.[6] One of the assumptions upon which this theory is based is that the principal contributor to the ionic strength is an inert electrolyte and that the reactant ions are present only in relatively low concentrations. Thus for conditions where this is not true, the results of such calculations must be considered as only approximate. Further, for this condition, the calculated ionic strength will depend on the concentrations of all the reactant ions which, in turn, depend on the ionic strength corrected equilibrium quotients. Thus iteration is required.

All of the log equilibrium quotients (log β's) were corrected for ionic strength using Specific ion Interaction Theory (SIT) according to equation 9. In equation 9, I_m is the ionic strength in moles/kg, Δz^2 is the difference in the sum of the squares of the ionic charges, and $\Delta\varepsilon$ is similarly defined in terms of the change in appropriate specific interaction coefficients, and n is the number of water molecules. The quantities $^*\beta_m$, and $^*\beta_0$ represent the formation constant of a complex in an ionic medium ($^*\beta_m$) or corrected to an ionic strength of zero ($^*\beta_0$). The log of the activity of water ($\log_{10} a_w$) is given by $-(2 \times 18 \times I_m/2303) \times OS$, where OS is the osmotic

Table 1. Thermodynamic Binding Constants for the Uranyl Carbonate System used in this study[a]

Ligand Data				$I_m = 0$	2.5	3.0
$CO_3^{2-} + H^+$	$\rightleftharpoons$	HCO_3^-	log K =	10.33	9.68	9.71
$CO_3^{2-} + 2H^+$	$\rightleftharpoons$	$CO_2\ (aq) + H_2O$	log K =	16.68	15.82	15.90
$HCO_3^- + H^+$	$\rightleftharpoons$	$CO_2\ (g) + H_2O$	log K =	7.82	7.65	7.70
Metal Complex Data						
$UO_2^{2+} + CO_3^{2-}$	$\rightleftharpoons$	$UO_2(CO_3)\ (aq)$	log β_{11} =	9.63	8.87	9.05
$UO_2^{2+} + 2\ CO_3^{2-}$	$\rightleftharpoons$	$UO_2(CO_3)_2^{2-}$	log β_{12} =	16.94	15.78	15.88
$UO_2^{2+} + 3\ CO_3^{2-}$	$\rightleftharpoons$	$UO_2(CO_3)_3^{4-}$	log β_{13} =	21.63	22.18	22.29
$3\ UO_2^{2+} + 6\ CO_3^{2-}$	$\rightleftharpoons$	$(UO_2)_3(CO_3)_6^{6-}$	log β_{36} =	54.00	55.32	55.59
Metal Hydrolysis Data						
$UO_2^{2+} + H_2O$	$\rightleftharpoons$	$UO_2(OH) + H^+$	log β_{1-1} =	-5.20	-4.71	-4.54
$2\ UO_2^{2+} + H_2O$	$\rightleftharpoons$	$(UO_2)_2(OH)^{3+}$	log β_{2-1} =	-2.70	-2.26	-2.25
$UO_2^{2+} + 2\ H_2O$	$\rightleftharpoons$	$UO_2(OH)_2 + 2H^+$	log β_{1-2} =	-10.30	-10.40	-10.34
$2\ UO_2^{2+} + 2\ H_2O$	$\rightleftharpoons$	$(UO_2)_2(OH)_2^{2+} + 2H^+$	log β_{2-2} =	-5.62	-6.05	-6.05
$3\ UO_2^{2+} + 4\ H_2O$	$\rightleftharpoons$	$(UO_2)_3(OH)_4^{2+} + 4H^+$	log β_{3-4} =	-11.90	-13.25	-13.36
$3\ UO_2^{2+} + 7\ H_2O$	$\rightleftharpoons$	$(UO_2)_3(OH)_7^- + 7H^+$	log β_{3-7} =	-31.00	-32.46	-32.60
$3\ UO_2^{2+} + 5\ H_2O$	$\rightleftharpoons$	$(UO_2)_3(OH)_5^+ + 5H^+$	log β_{3-5} =	-15.55	-16.74	-16.74
$4\ UO_2^{2+} + 7\ H_2O$	$\rightleftharpoons$	$(UO_2)_4(OH)_7^+ + 7H^+$	log β_{4-7} =	-21.90	-23.17	-23.10

[a] Values at $I_m = 0$ taken from NEA review (reference 6) and corrected using SIT

coefficient of the solution. The osmotic coefficients were estimated to be the same as for $NaClO_4$ as given in Robinson and Stokes.[50] Quadratic equations for OS as a function of concentration were fit to two concentration regions: $0.4 \text{ m} \le I_m \le 1.0 \text{ m}$, and $1.0 \text{ m} \le I_m \le 4.0 \text{ m}$.

$$\log_{10} {}^*\beta_m = \log_{10} {}^*\beta_0 + \Delta z^2 \left(\frac{0.5091\sqrt{I_m}}{1 + 1.5\sqrt{I_m}} \right) - \Delta\varepsilon(I_m) + n \log_{10} a_w \qquad (9)$$

2.3.3 Hydrogen ion concentration; pH vs p[H]. The final step prior to data analysis is the accurate determination of the quantity -log[H+], which we will refer to as p[H] in order to distinguish from the approximate value known as pH.[9] While the pH scale is widely used throughout the Yucca Mountain Site Characterization Project as a measure of acidity or alkalinity of aqueous solutions, this should only be done with the understanding that the pH values obtained are *approximate* and that they cannot be precisely measured or explicitly defined.[51,52] In spite of the fact that pH measurement is now a matter of routine, the fundamentals governing it are not widely understood. It is fundamentally impossible to measure exactly the activity of an individual ionic species because they never occur alone. Cations and anions are always present in pairs, and together they make up the ionic strength of solution. This is the problem with the pH scale, since pH is defined as a measure of the activity of hydrogen ions: pH = -log(a_{H+}). But this itself is a function of the ionic strength. The ionic strength effect on the pH of a buffer solution has been demonstrated by Feldman.[53] Feldman showed that the pH of a 0.05 M potassium hydrogen phthalate solution can vary by as much as 0.5 pH units as a function of added KCl. It is quite evident that the decrease in pH is due mainly to changing activity coefficients with subsequent increased dissociation of the week acid.

In order to evaluate thermodynamic data, it is important to know -log[H+] with a reasonable degree of precision. Using the equilibrium constants accepted by the NEA for the reactions shown in equations 10 - 12 one can readily calculate p[H] = -log[H+] as a function of ionic strength from first principles. Buffer solutions were prepared by equilibrating solutions of

NaClO$_4 \cdot$H$_2$O and NaHCO$_3$ with CO$_2$ gas mixtures of known compositions at an ionic strength of interest. The compositions of synthetic buffers prepared at I_m = 2.3 and 3.0 m is given in Table 2. All buffers were transferred to gas scrubbers and attached to appropriate certified gas mixtures and allowed to bubble under known partial pressures of CO$_2$. Carbon dioxide gas was humidified by bubbling through a 3.0 mol/kg KCl solution prior to passing over samples in order to maintain a constant vapor pressure and minimize evaporation of sample solutions. The pH electrode was calibrated with commercial pH buffer solutions, and then pH readings of our synthetic buffers were recorded after 48, 72, and 120 hrs and found to be stable. A plot of experimentally measured pH versus calculated p[H] is shown in Figure 10 for ionic strengths of 3.0 and 2.5 moles/kg. It is significant to note that at these ionic strengths, pH and p[H] values can differ by nearly 0.6 log units.

$$CO_3^{2-} + H^+ \rightleftharpoons HCO_3^- \tag{10}$$

$$CO_3^{2-} + 2H^+ \rightleftharpoons CO_2 (aq) + H_2O \tag{11}$$

$$H^+ + HCO_3^- \rightleftharpoons CO_2 (g) + H_2O \tag{12}$$
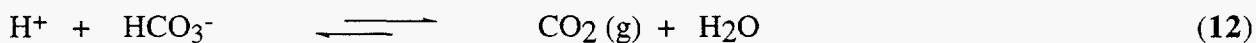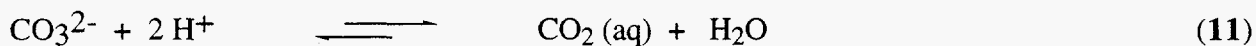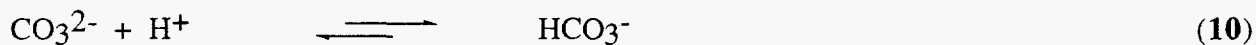
2.3.4 Species Distributions Determined by Multinuclear NMR. A species distribution plot for the uranyl carbonate system including hydrolysis and based on the NEA suggested data corrected to I_m = 2.5 m is shown in Figure 11. The concentration of uranyl and carbonate ligands correspond to those used in the ^{13}C NMR experiment at I_m = 2.5 m. The species distribution predicted by the suggested NEA binding constants can be compared with the experimentally observed species distribution based on ^{13}C NMR integration. Carbon-13 NMR integration data obtained at I_m = 2.5 m are given in Table 3 as a function p[H]. The observed and calculated species distributions for this ^{13}C data as a function of p[H] is shown in Figure 12. The p[H] range in figure 12 runs between $7.0 \leq$ p[H] ≤ 10.0 since this is the region of sample preparation where stable p[H] values were obtained, and no CO$_2$ was flushed through the NMR

28

Table 2. Composition of Synthetic CO_3^{2-}/HCO_3^- buffer solutions at I_m = 3.0 and 2.5 m for p[H] determination

[NaClO4]	[NHCO3]	mm Hg	f-CO2	I_m.	ρ (g/ml)	p[H]	pH
2.4415	0.2000	570	0.03	3.000	1.20	8.7041	8.08
2.4415	0.2002	570	0.302	2.977	1.20	7.7599	7.22
2.5998	0.1002	570	1.0	3.105	1.20	6.9782	6.40
2.6221	0.0103	570	1.0	3.038	1.19	5.9875	5.40
2.0403	0.2000	570	0.03	2.524	1.16	8.6513	8.11
2.0501	0.2000	570	0.302	2.525	1.16	7.7105	7.23
2.1500	0.1001	570	1.0	2.505	1.17	6.8893	6.40
2.2300	0.0100	570	1.0	2.500	1.17	5.8917	5.44
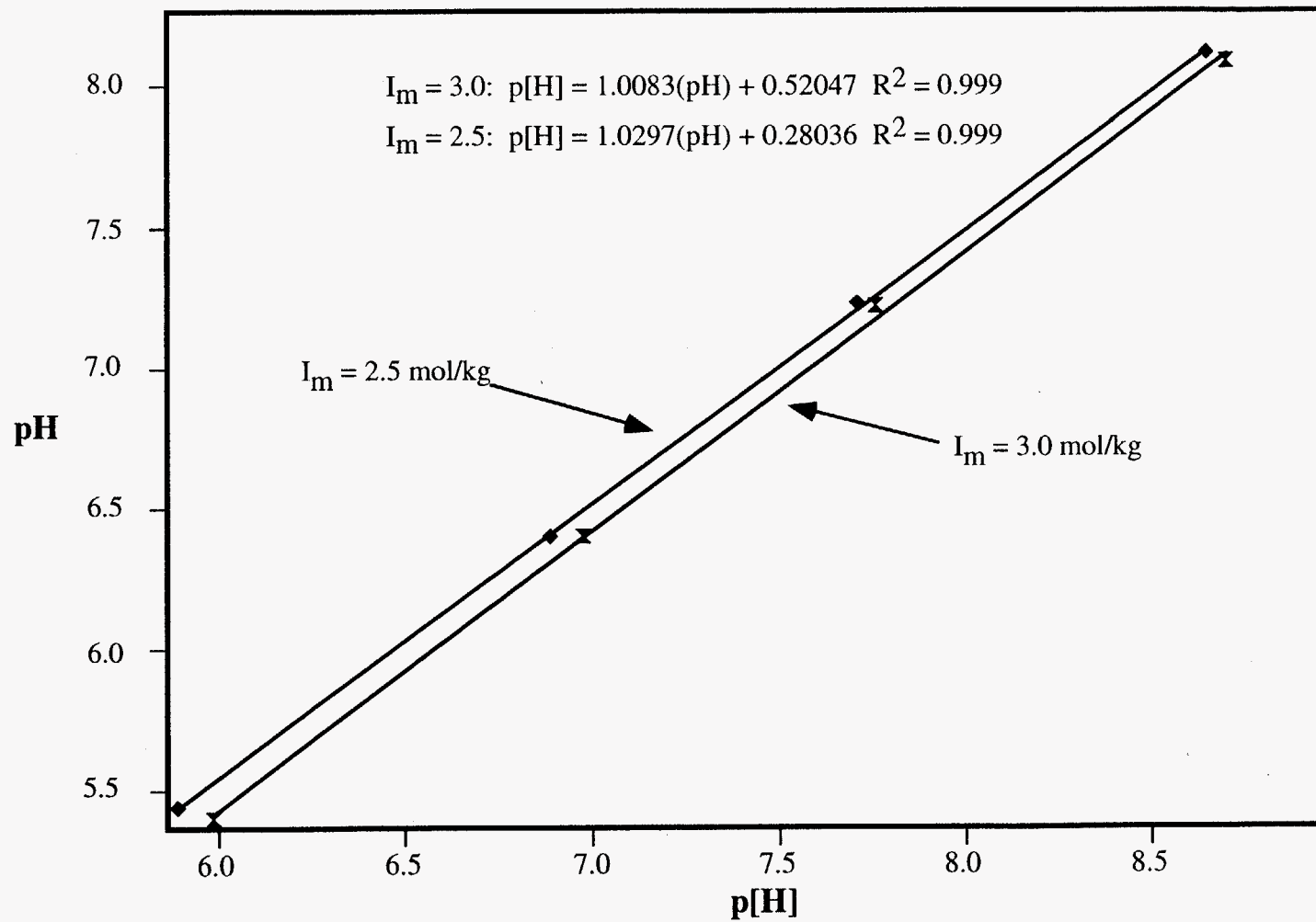
Figure 10. Calibration graph showing pH versus p[H] determined from synthetic buffer solutions at ionic strengths of 2.5 and 3.0 moles/kg.
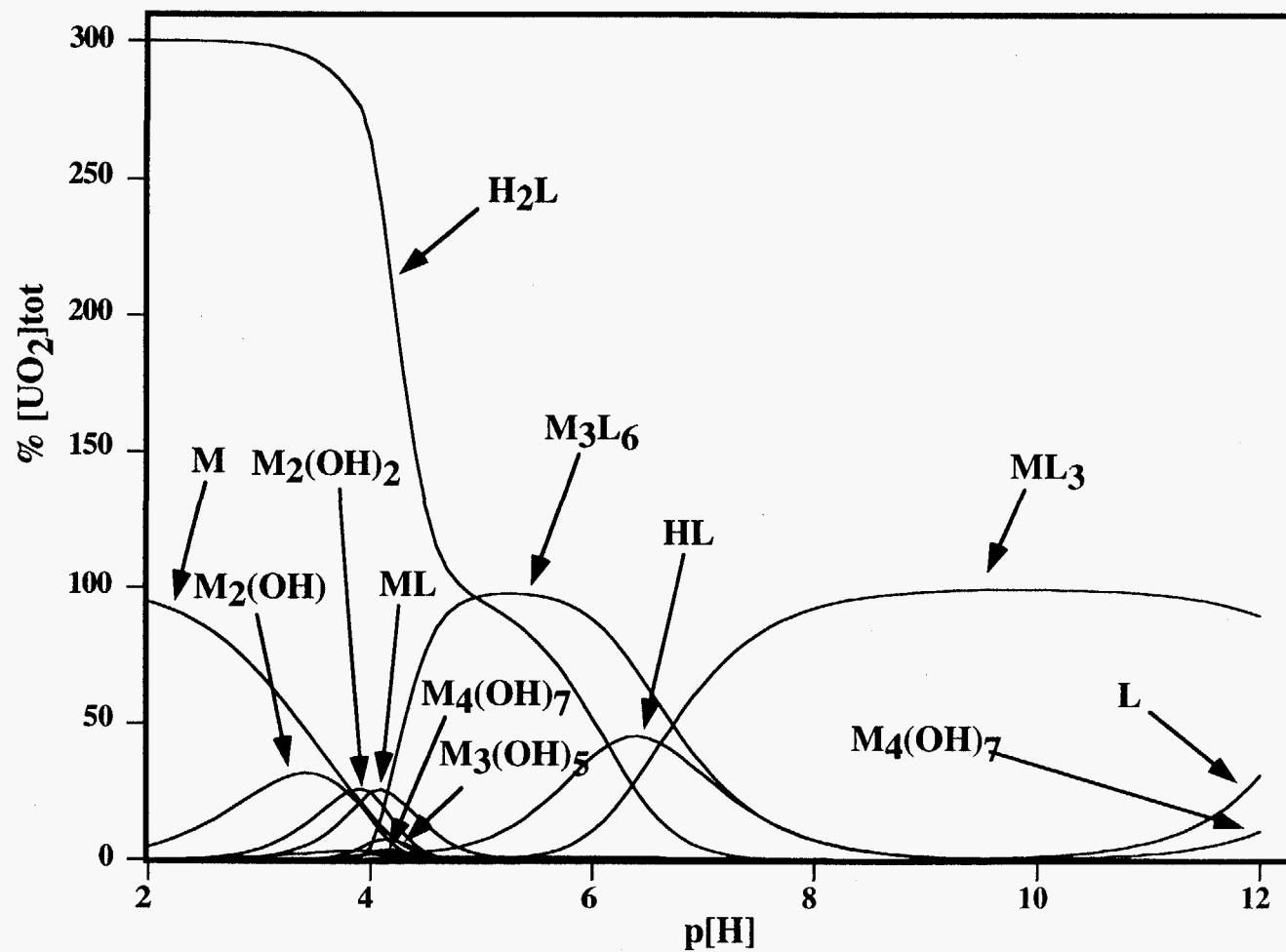
Figure 11. Calculated uranyl species distribution using suggested NEA binding constants corrected to $I_m = 2.5$ m. Concentrations correspond to ^{13}C NMR data with $[UO_2^{2+}] = 0.05$ M, $[CO_3^{2-}/HCO_3^-] = 0.15$ M. Major species are indicated on graph where $M = UO_2$ and $L = CO_3^{2-}$.

Table 3. ^{13}C NMR Integrations for CO_3^{2-} containing species at 6°C and $I_m = 2.5$ m

p[H]	δ 166.2	δ 165.2	δ 164.9	% $(UO_2)_3(CO_3)_6^{6-}$	% $UO_2(CO_3)_3^{4-}$
9.826	0	1.0	0	0	100
8.659	1.0	208.42	1.0	0.5	99.5
8.440	1.0	119.07	1.0	0.8	99.2
8.282	1.0	48.44	1.0	2	98
8.122	1.0	34.12	1.0	3	97
8.037	1.0	35.11	1.0	3	97
7.957	1.0	14.48	1.0	6.5	93.5
7.856	1.0	11.46	1.0	8	92
7.738	1.0	5.49	1.0	15.4	84.6
7.498	1.0	6.29	1.0	13.7	86.3
7.357	1.0	5.20	1.0	16.2	83.8
7.260	1.0	2.62	1.0	27.6	72.4
6.987	1.0	1.0	1.0	50	50
6.997	1.0	0.53	1.0	65.4	34.6
6.785	1.0	0.28	1.0	78.1	21.9

Figure 12. Calculated (solid line) and experimental (data points) uranyl species distribution using suggested NEA binding constants corrected to I_m = 2.5 m. Concentrations correspond to ^{13}C NMR data with $[UO_2^{2+}]$ = 0.05 M, $[CO_3^{2-}/HCO_3^-]$ = 0.15 M. Monomer and trimer species are indicated on figure where M = UO_2 and L = CO_3^{2-}.

samples. The species distributions for the uranyl carbonate system as observed by multinuclear NMR agree well with the NEA predictions, demonstrating the applicability of NMR to speciation studies, and validating the suggested NEA values. This is especially important for the trimeric $(UO_2)_3(CO_3)_6^{6-}$ complex. The five determinations for $\log\beta_{36}$ used by the NEA in their evaluation were not consistent, and the review selected the unweighted average of these values.[6] While the data in Figure 12 shows that the value of $\log\beta^0_{36} = 54.0 \pm 1.0$ gives a reasonably good fit to the observed data, the direct observation of this species by multinuclear NMR provides the opportunity to refine this value.
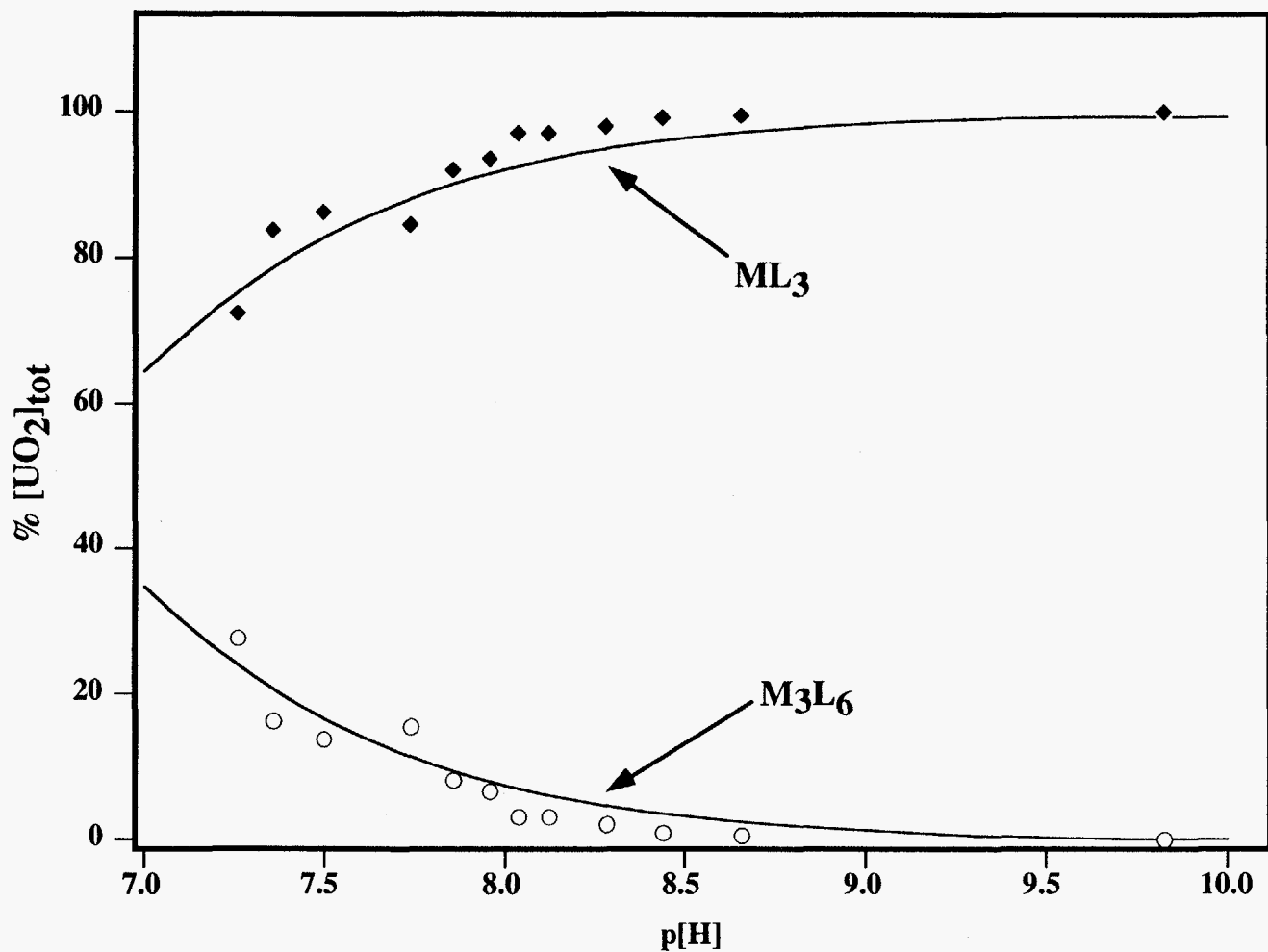
The experimental observables in the NMR experiment are $[UO_2(CO_3)_3^{4-}]$, $[(UO_2)_3(CO_3)_6^{6-}$, and $[HCO_3^-]$. From electrode calibration, we know $[H^+]$, and hence all the concentrations in equation 13 are known. From these concentrations, one can calculate the equilibrium constant for equation 13 at $I_m = 2.5m$ and $25°C$ to be $\log K = 17.9(\pm0.8)$. In order to compare this valve with the NEA suggestions, we can use Specific Ion Interaction theory to calculate the equilibrium constants for the equilibria shown in equations 14 and 15 at $I_m = 2.5m$. These values are given in Table 1.

$$3UO_2(CO_3)_3^{4-} + 3H^+ \rightleftharpoons (UO_2)_3(CO_3)_6^{6-} + 3HCO_3^- \tag{13}$$

$$UO_2^{2+} + 3CO_3^{2} \rightleftharpoons UO_2(CO_3)_3^{4-} \tag{14}$$

$$HCO_3^- \rightleftharpoons H^+ + CO_3^{2-} \tag{15}$$

$$3UO_2^{2+} + 6CO_3^{2-} \rightleftharpoons (UO_2)_3(CO_3)_6^{6-} \tag{16}$$
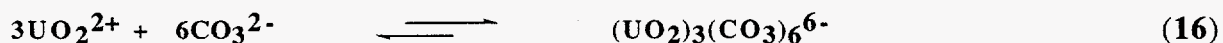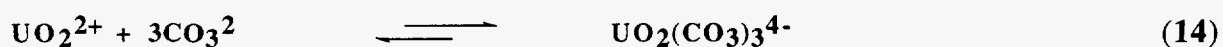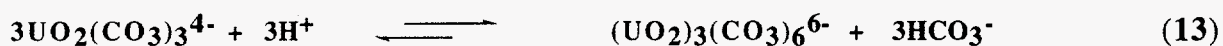
By a simple addition of equation 13 to three times equation 14 and three times equation 15, we derive equation 16 with an experimental $\log\beta_{36} = 55.40(\pm0.8)$ at $I= 2.5m$. From Table 1, we see that the NEA pediction is $55.32(\pm1.0)$. The agreement is excellent.

2.4 Calculated Uranyl Species Distributions in Yucca Mountain Groundwaters.
Since we have shown that the thermodynamic data suggested by the NEA can be validated by multinuclear NMR spectroscopy, we can now use these thermodynamic binding constants to examine the species distributions in groundwater found at the proposed Yucca Mountain repository. Chemical analyses have established that the Yucca Mountain groundwaters are primarily sodium bicarbonate containing waters with very little dissolved solids.[54,55] Sodium is by far the dominant cation. The water from the J-13 well is thought to be representative of fracture and interstitial waters in the Yucca Mountain Tuff and has been recommended as a reference water.[56] Carbonaceous water from UE-25P#1 has an order of magnitude more carbonate than the J-13 well and thus represents a possible upper bound for carbonate concentrations. Thus we can assume a boundary condition of carbonate ligand concentrations between 0.001 and 0.01 M for these two waters.

Thermodynamic binding constants listed in Table 1 were adjusted to an ionic strength of 0.002 moles/kg using SIT and species distributions in J-13 groundwater were calculated. The initial uranyl cation concentrations were increased over several orders of magnitude to determine the impact of uranyl ion concentrations of 1×10^{-5}, 1×10^{-4}, and 1×10^{-3} mole/liter. The ionic strength was then corrected to an ionic strength of 0.01 moles/kg and the species distribution calculated for a uranyl concentration of 0.01 mole/liter. These species distribution plots for various concentrations of uranyl ion in J-13 groundwater are shown in Figures 13 and 14. Thermodynamic binding constants adjusted to an ionic strength of 0.01 moles/kg were used to calculate species distributions in UE-25P#1 groundwater for uranyl concentrations of 1×10^{-5}, 1×10^{-4}, and 1×10^{-3} mole/liter. The binding constants were then corrected to an ionic strength of 0.02 moles/kg and the species distribution calculated for a uranyl concentration of 0.01 mole/liter. These species distribution plots for various concentrations of uranyl ion in UE-25P#1 groundwater are shown in Figures 15 and 16.

From the species distribution plots shown in Figures 13 - 16 it is clear that in both J-13 and UE-25P#1 groundwaters, the chemistry of the uranyl ion is markedly influenced by carbonate complexation at low uranyl ion concentration. Monomeric uranyl carbonate species including $UO_2(CO_3)$, $UO_2(CO_3)_2{}^{2-}$, and $UO_2(CO_3)_3{}^{4-}$ predominate above p[H] 4 - 6, and hydrolysis to form $UO_2(OH)_3{}^-$ is predicted to dominate at high p[H] values near 11.0. Carbonate complexation dominates the speciation for the uranyl ion as long as there is ample carbonate present in solution. When the metal ion concentration exceeds the carbonate concentration, then hydrolysis begins to play an important role. This is easily seen in Figures 13 and 14 for J-13 groundwater, where the carbonate ion is only present in concentrations of 0.002 M. One sees from the figures that carbonate complexation dominates the speciation for uranyl concentrations of 10^{-5} and 10^{-4} M (Figure 13) but hydrolysis begins to become important when the uranyl ion concentration exceeds the carbonate ion concentration, such as seen for uranyl concentrations 10^{-3} and 10^{-2} M (Figure 14). This same scenario is predicted for UE-25P#1 groundwater, except that carbonate complexation dominates the speciation over a larger range of uranyl ion concentrations. Since the carbonate concentration in UE-25P#1 groundwater is 0.0114 M, carbonate complexation is much more prevalent covering a uranyl concentration range of 10^{-5} - 10^{-3} M (Figures 15 and 16). It is significant that the two species observed by multinuclear NMR spectroscopy in this study, $UO_2(CO_3)_3{}^{4-}$ and $(UO_2)_3(CO_3)_6{}^{6-}$, are both predicted to be important species in UE-25P#1 groundwater at $10^{-3}M$ uranyl concentrations and higher (Figure 16). It is instructive to compare the J-13 and UE-25P#1 species distributions on the same diagram. Figure 17 shows a comparison of uranyl carbonate and hydrolyzed uranyl species in both groundwaters. Hydrolysis and carbonate complexation have been separated into two distinct groupings for comparison. As expected, the higher carbonate concentration in UE-25P#1 water suppresses hydrolysis in favor of carbonate complexation as seen in the figure.
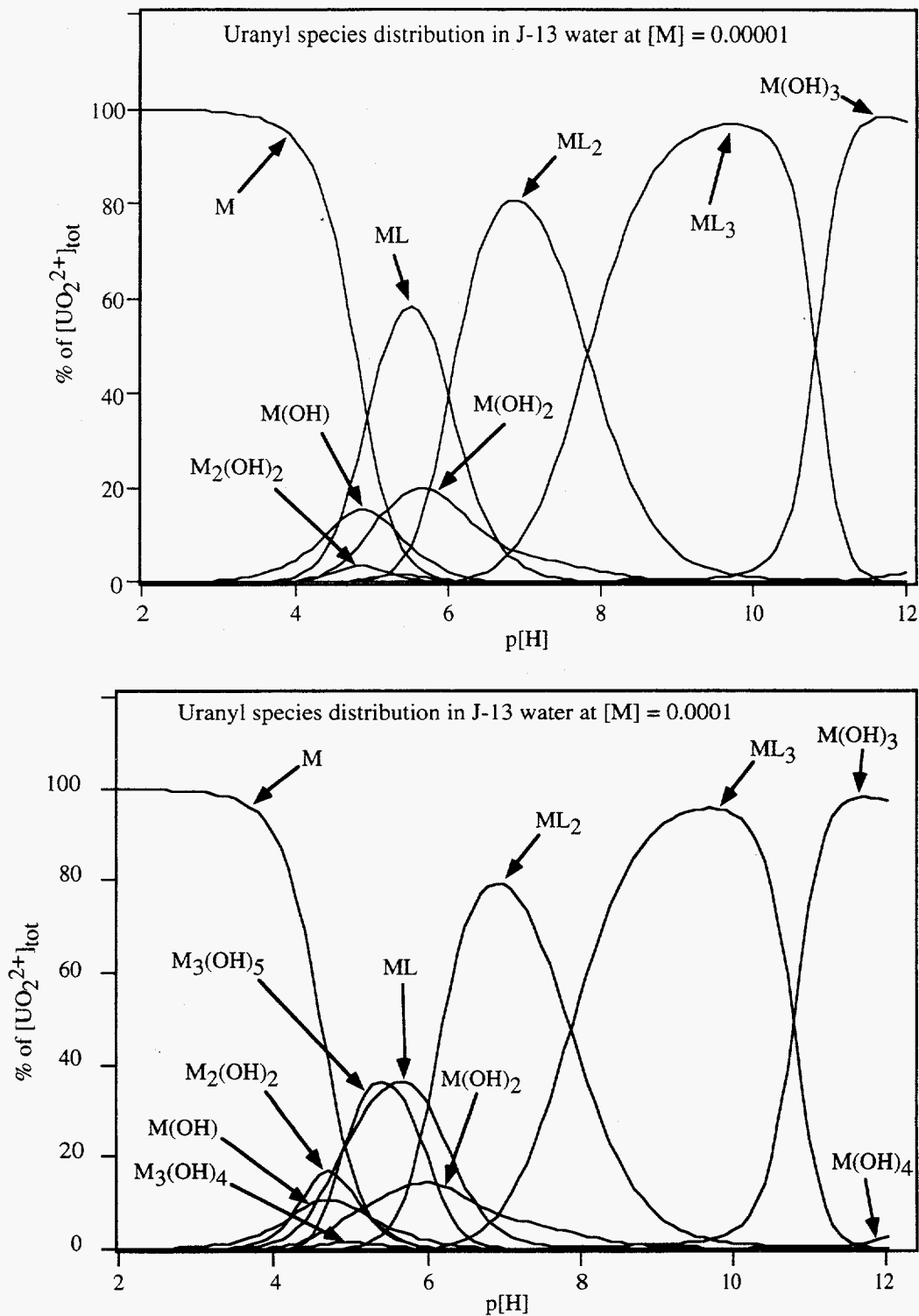
Figure 13. Uranyl species distribution in J-13 groundwater using NEA thermodynamic binding constants at I_m = 0.002 molal with uranyl concentrations of 0.00001 M (top) and 0.0001 M (bottom). M = UO_2^{2+} and L = CO_3^{2-}.
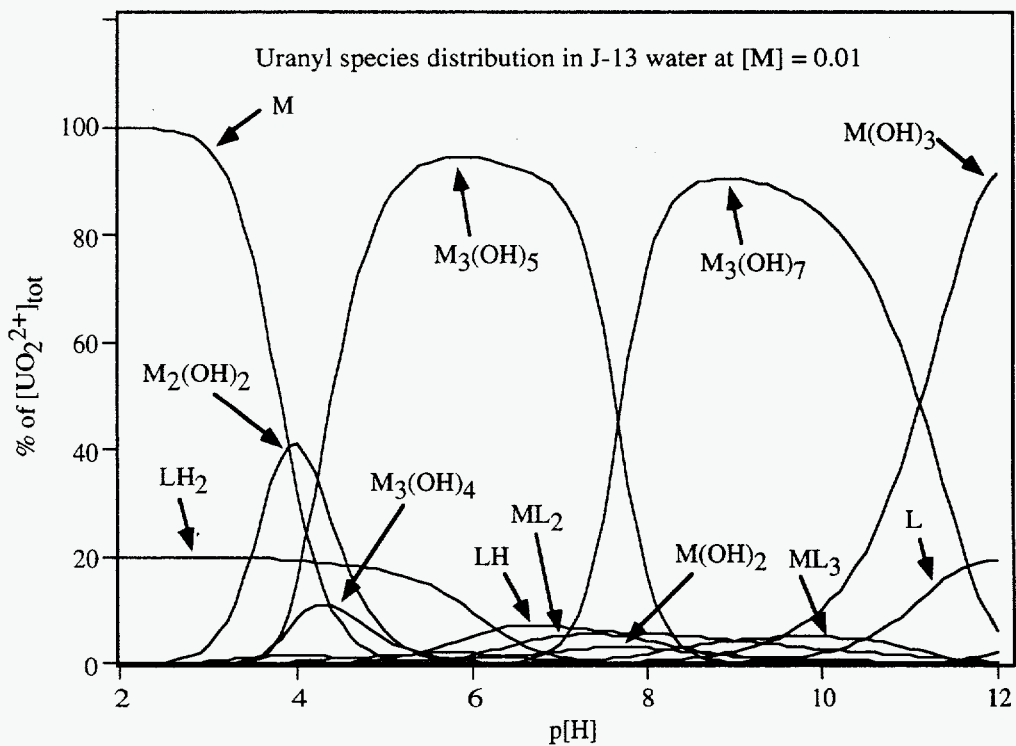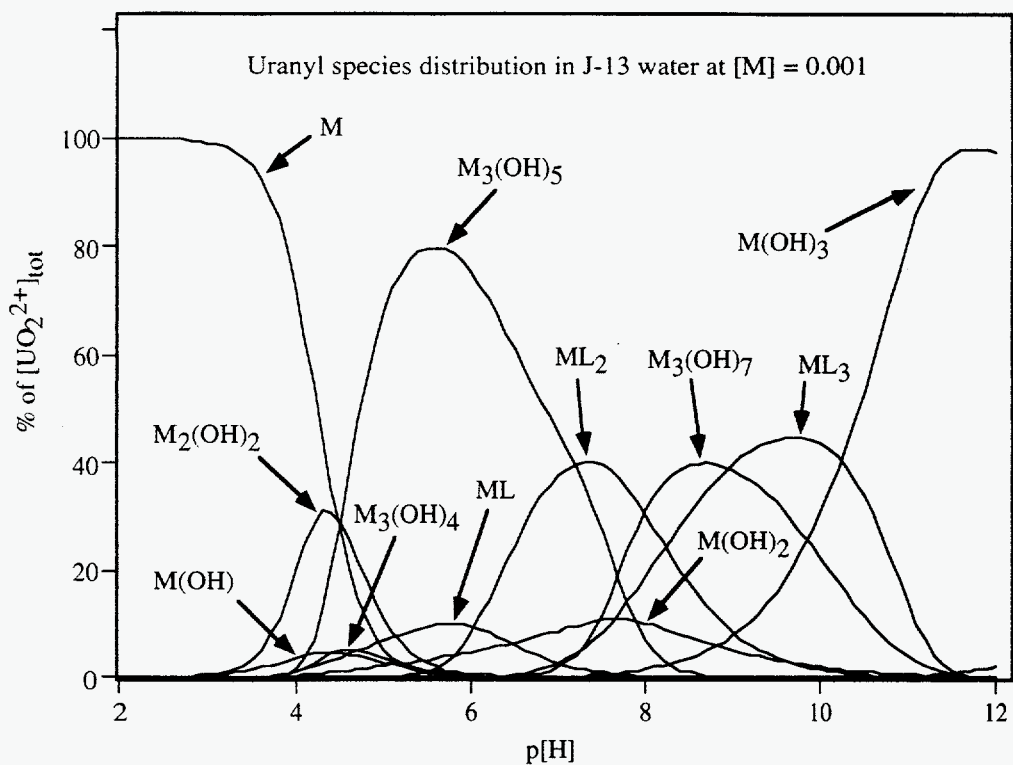
Figure 14. Uranyl species distribution in J-13 groundwater using NEA thermodynamic binding constants at $I_m = 0.002$ molal with a uranyl concentration of 0.001 M (top) and at $I_m = 0.01$ with a uranyl concentration of 0.01 M (bottom). $M = UO_2^{2+}$ and $L = CO_3^{2-}$.

Figure 15. Uranyl species distribution in UE-25P#1 groundwater using NEA thermodynamic binding constants at $I_m = 0.01$ molal with uranyl concentration of 0.00001 M (top) and 0.0001 M (bottom). $M = UO_2^{2+}$ and $L = CO_3^{2-}$.

39

Figure 16. Uranyl species distribution in UE-25P#1 groundwater using NEA thermodynamic binding constants at $I_m = 0.01$ molal with a uranyl concentration of 0.001 M (top) and at $I_m = 0.02$ with a uranyl concentration of 0.01 M (bottom). $M = UO_2^{2+}$ and $L = CO_3^{2-}$.
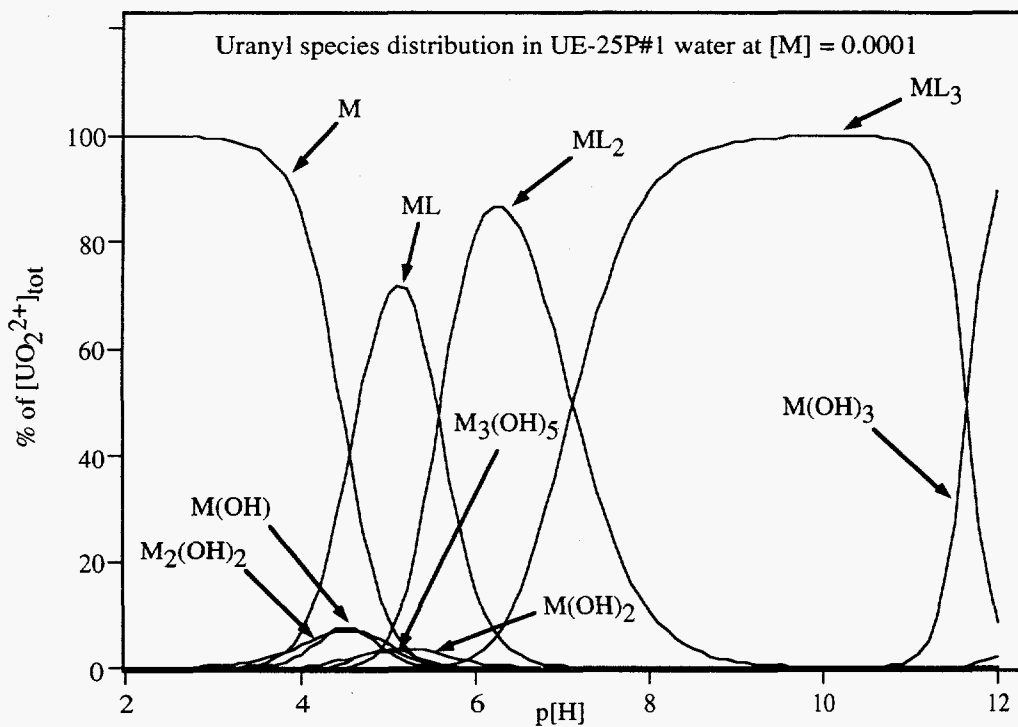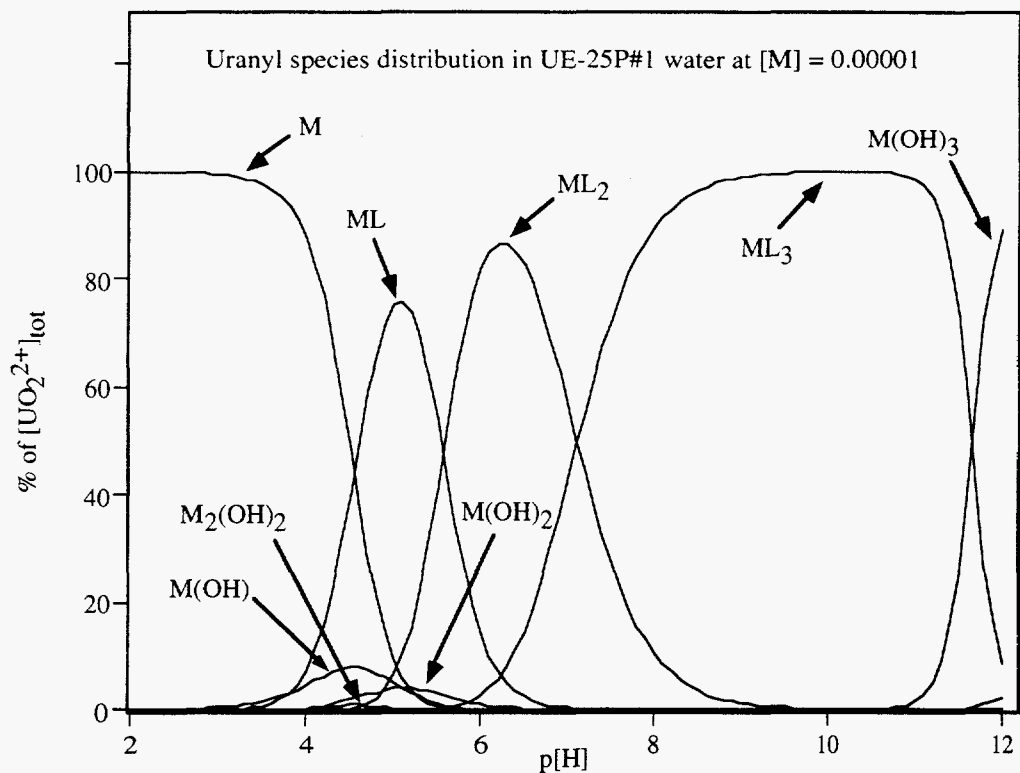
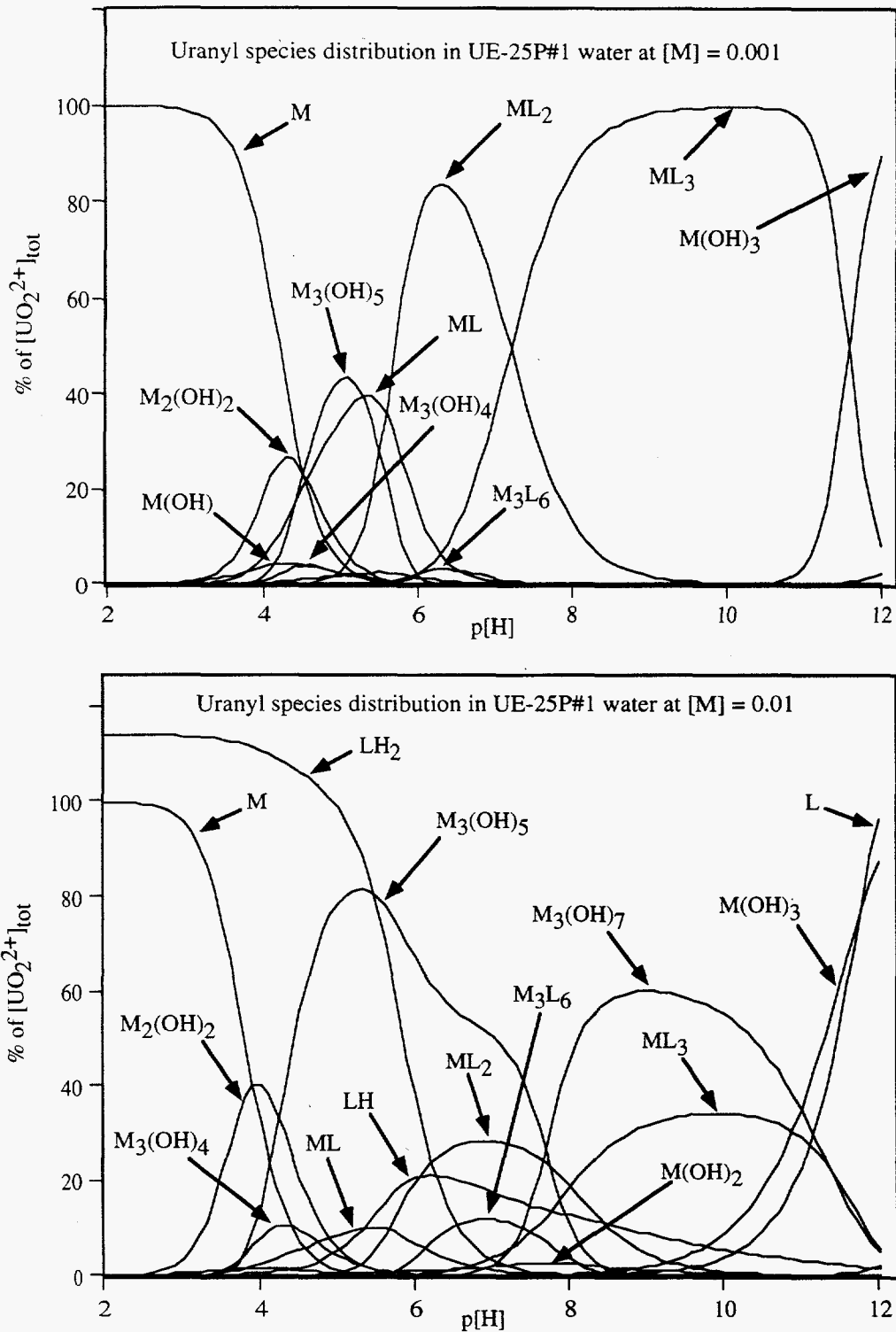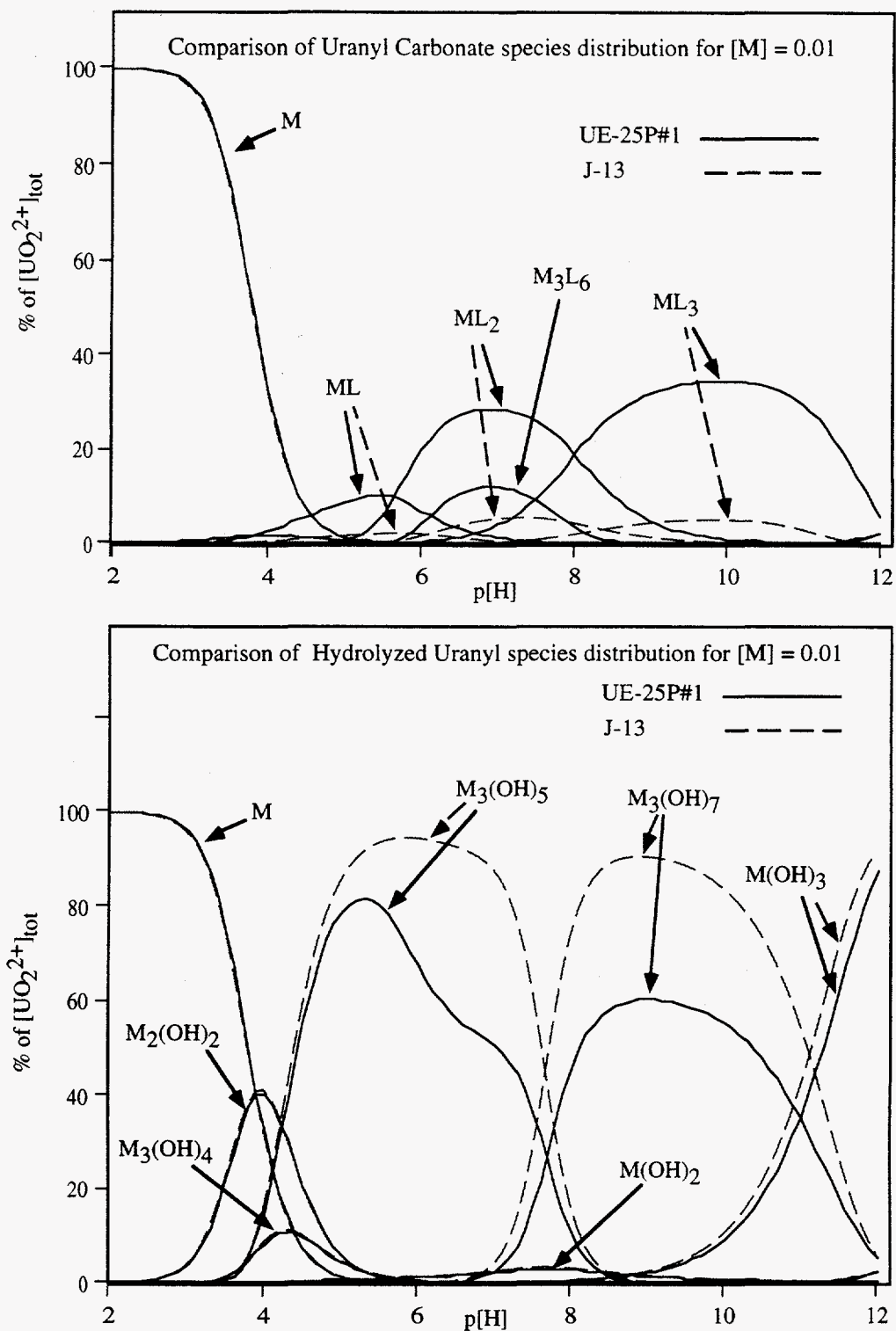**Figure 17.** Comparison of uranyl species distribution in UE-25P#1 and J-13 groundwater using NEA thermodynamic binding constants at $I_m = 0.02$ with a uranyl concentration of 0.01 M. Carbonate complexation is compared in the top figure, and hydrolysis is compared in the bottom figure. $M = UO_2^{2+}$ and $L = CO_3^{2-}$.

41

3.0 Concluding Remarks

These ^{13}C and ^{17}O NMR studies establish that synthetic isotopic enrichment of actinyl carbonate complexes can readily be achieved, and demonstrate the viability of multinuclear NMR as a *species-specific* probe for solution speciation studies in near-neutral solution. Other, more traditional approaches to speciation require that potentiometric, coulombic, or absorption spectrophotometric data be fit to a numerical model and refined using nonlinear least-squares. The preferred method for measurement and refinement of equilibrium constants is still potentiometric titration, and curve-fitting the data to a set of thermodynamic constants. However, the computer programs used in the fitting are so prevalent and easy to use that in some cases, too many species have been used to fit the observed data, that the resulting parameters are meaningless. The problems of low-quality data and putative species makes it necessary from a quality assurance standpoint to have alternate methods available with which to test the validity of the available data. The multinuclear NMR approach allows the different species to be observed directly, thereby removing much ambiguity in assignment of relevant species present in solution. Concentrations are easily extracted from the data by integration, and thermodynamic binding constants can be assessed. This demonstrates that multinuclear NMR spectroscopy will be an invaluable *species-specific* tool for determination of new or unknown binding constants for the transuranium elements.

Uranium(VI) is by far the most well-studied actinide system available, and the NEA review of the uranium(VI) literature appears to have done an outstanding job of picking through this data and suggesting a suitable set of thermodynamic constants for hydrolysis and carbonate complexation of uranium(VI). This NMR study serves to validate these thermodynamic constants. It is also quite clear that with fewer studies available for the corresponding neptunium, plutonium, and americium systems, the linear regression of the available data to $I_m = 0$ will be far more difficult, and accurate studies of the thermodynamic binding constants for these elements is still badly needed. We believe that future multinuclear NMR studies of the important transuranic

systems will provide invaluable insight for choosing the best model to fit new and existing potentiometric and spectrophotometric titration data. This should provide the most accurate estimate of thermodynamic constants for use in geochemical, site assessment, and performance assessment modeling. Along these lines, we have already begun scoping studies into Np(VI) and Np(V) carbonate complexation by multinuclear NMR, and have observed both $NpO_2(CO_3)_3^{4-}$ and $(NpO_2)_3(CO_3)_6^{6-}$ species by ^{13}C NMR spectroscopy.

4.0 Experimental Section.

4.1 General considerations. All manipulations were carried out inside fume hoods or negative pressure gloveboxes designed for containment of radioactive materials in a laboratory equipped with appropriate safeguards for manipulation of such materials (monitoring devices, HEPA-filtered ventilation, etc.). Personnel wore lab coats and surgical gloves at all times. Radioactive wastes were handled in accordance with Los Alamos waste management practices and policies. Sodium perchlorate monohydrate was purchased from Fluka and used without purification. Sodium carbonate, sodium bicarbonate, and guanidine carbonate were obtained from Aldrich and used without further purification. D_2O (99.9 % D) and ^{13}C-enriched Na_2CO_3 (99.9 % ^{13}C) were purchased from Cambridge Isotopes. Deuterium oxide was degassed by bubbling with argon for 1 hr, and the $Na_2^{13}CO_3$ was used as received. ^{17}O-enriched H_2O (20 % ^{17}O) was obtained from Los Alamos National Laboratory Stock, and used without further purification. $UO_2(ClO_4)_2(H_2O)_6$ was recrystallized 3 times. Ozone was prepared in an OREC model 03V10-O Ozone Generator. pH was measured with a Corning model 130 pH meter and an ORION model 8103 ROSS combination electrode. Carbon dioxide gas was humidified by bubbling through a 3.0 *M* KCl solution prior to passing over samples in order to maintain a constant vapor pressure and minimize evaporation of sample solutions.

4.2 *Spectrophotometric Measurements*. Solution UV-visible-NIR spectra were recorded using a Perkin-Elmer Lambda 9 in matched 1.0 or 0.1 cm quartz cells. Extinction coefficients were measured from the baseline.

4.3 *Electrochemical Preparations*. Electrochemical synthesis of [17]O-labeled actinide solutions were performed using an EG&G Parr Model 173 potentiostat/coulometer. Electrochemical cells used for bulk electrolysis had separate compartments for reference and counter-electrodes and are described in detail elsewhere.[57] A Pt screen working electrode was separated from a Pt wire counter electrode by a Vicor frit, and a saturated calomel electrode (SCE) was employed.

4.4 *NMR Measurements*. All NMR sample solutions were loaded into Wilmad 5mm o.d. 507-PP Pyrex glass NMR tubes which were flame-sealed with a small hand torch. Variable-temperature FT ^{13}C and ^{17}O NMR spectra were recorded on a Bruker AF 250 spectrometer fitted with a 5mm selective probehead operating at 62.9 or 33.9 MHz, or on a Varian Unity 300 spectrometer with a 5mm selective probehead operating at 40.7 MHz with ^{2}H field-frequency lock. The [13]C $\pi/2$ pulse length was measured to be 5.25 μs using the free carbonate resonance. The temperature was controlled with a Bruker variable temperature controller and was stable to within ± 1K. The temperature was determined by measurement of the ^{1}H NMR of ethylene glycol (295 - 350 K) or methanol (270 -295 K) at the same temperature and gas flow rate. All ^{13}C NMR chemical shifts are reported in ppm relative to the carbonyl carbon of external acetone-d_6 set at $\delta = 206.0$. All ^{17}O NMR chemical shifts are reported in ppm relative to external H_2O set at $\delta = 0$.

4.5 *Preparation of bicarbonate p[H] buffers*. Buffer solutions were prepared by equilibrating solutions of $NaClO_4$ and $NaHCO_3$ with CO_2 gas mixtures of known compositions. All buffers were transferred to gas scrubbers and hooked up to appropriate certified gas mixtures

44

and allowed to bubble. p[H] readings were recorded after 48, 72, and 120 hrs and were found to be stable. An Orion Ross Combination electrode was calibrated with commercial buffers at pH=7 and pH=10 on an Orion ion analyzer before readings were taken. Density readings for each synthetic buffer were obtained by weighting 10 ml of each solution. A barometric pressure of 570 mm Hg (7,300 ft above sea level) was used.

Ionic strength 3.0 m buffer. p[H] was plotted against pH and linear regression gave the following correction for experiments at an ionic strength I_m = 3.0 mol/kg. p[H] = 1.00828(pH) + 0.520468, R^2 = 0.9996. Buffer #1, p[H] 8.70. 27.34 ml of 8.93M $NaClO_4$ solution (244.15 mmol), and 1.6803 g (20.00 mmol). of $NaHCO_3$ were combined and brought to the mark in a 100 mL volumetric flask to give a solution of composition 2.4415 M $NaClO_4$, 0.2 M $NaHCO_3$, ρ = 1.2013 g/mL, and I = 3.00 mol/kg. This solution was bubbled with 3% (f-CO_2 = 0.03) CO_2-Ar to establish equilibrium. Buffer #2, p[H] 7.76. 27.34 ml of 8.93 M $NaClO_4$ solution (244.15 mmol), and 1.6818 g (20.02 mmol) of $NaHCO_3$ were combined and brought to the mark in a 100 mL volumetric flask to give a solution of composition 2.4415 M $NaClO_4$, 0.2002 M $NaHCO_3$, ρ = 1.2039 g/mL, and I = 2.98 mol/kg. This solution was bubbled with 30.2% (f-CO_2 = 0.302) CO_2-Ar to establish equilibrium. Buffer #3, p[H] 6.98. 36.5121 g (259.95 mmol) of $NaClO_4 \cdot H_2O$ and 0.8419 g (10.02 mmol) of $NaHCO_3$ were combined and brought to the mark in a 100 mL volumetric flask to give a solution of composition 2.5998 M $NaClO_4$, 0.1002 M $NaHCO_3$, ρ = 1.1964 g/mL, and I = 3.10 mol/kg. This solution was bubbled with 100% (f-CO_2 = 1.0) CO_2 to establish equilibrium. Buffer #4, p[H] 5.99. 36.8247 g (262.27 mmol). of $NaClO_4 \cdot H_2O$ and 0.0869 g (1.03 mmol) of $NaHCO_3$ were combined and brought to the mark in a 100 mL volumetric flask to give a solution of composition 2.6221 M $NaClO_4$, 0.0103 M $NaHCO_3$, ρ = 1.1886 g/mL, and I = 3.04 mol/kg. This solution was bubbled with 100% (f-CO_2 = 1.0) CO_2 to establish equilibrium.

Ionic strength 2.5 m buffer. p[H] was plotted against pH and linear regression gave the following correction for experiments at an ionic strength I_m = 2.5 mol/kg. p[H] =

1.00828(pH) + 0.520468, R^2 = 0.9999. Buffer #1, p[H] 8.65. 28.6538 g (204 mmol) of $NaClO_4 \cdot H_2O$, and 1.6800 g (20 mmol) of $NaHCO_3$ were combined and brought to the mark in a 100 mL volumetric flask to give a solution of composition 2.0403 M $NaClO_4$, 0.2 M $NaHCO_3$, ρ = 1.16 g/mL, and I = 2.52 mol/kg. This solution was bubbled with 3% (f-CO_2 = 0.03) CO_2-Ar to establish equilibrium. Buffer #2, p[H] 7.71. 28.795 g (205 mmol) of $NaClO_4 \cdot H_2O$, and 1.6800 g (20 mmol) of $NaHCO_3$ were combined and brought to the mark in a 100 mL volumetric flask to give a solution of composition 2.0501 M $NaClO_4$, 0.2 M $NaHCO_3$, ρ = 1.16 g/mL, and I = 2.52 mol/kg. This solution was bubbled with 30.2% (f-CO_2 = 0.302) CO_2-Ar to establish equilibrium. Buffer #3, p[H] 6.89. 30.1993 g (215 mmol) of $NaClO_4 \cdot H_2O$, and 0.8412 g (10 mmol) of $NaHCO_3$ were combined and brought to the mark in a 100 mL volumetric flask to give a solution of composition 2.150 M $NaClO_4$, 0.1001 M $NaHCO_3$, ρ = 1.17 g/mL, and I = 2.51 mol/kg. This solution was bubbled with 100% (f-CO_2 = 1.0) CO_2-Ar to establish equilibrium. Buffer #4, p[H] 5.89. 31.3225 g (223 mmol) of $NaClO_4 \cdot H_2O$, and 0.084 g (1 mmol) of $NaHCO_3$ were combined and brought to the mark in a 100 mL volumetric flask to give a solution of composition 2.230 M $NaClO_4$, 0.010 M $NaHCO_3$, ρ = 1.17 g/mL, and I = 2.50 mol/kg. This solution was bubbled with 100% (f-CO_2 = 1.0) CO_2-Ar to establish equilibrium.

4.6 Solution Preparations. ^{17}O - enriched solutions.

Single crystals of $UO_2(ClO_4)_2(H_2O)_6$ (0.577 g, 1.0 mmol) were dissolved in 2.5 mL of 20.4% $H_2^{17}O$ and 0.250 mL of 10.7 M ultra-pure $HClO_4$ to prepare a 20% ^{17}O-enriched solution of 0.4 M UO_2^{2+} ion in 1M $HClO_4$. This uranyl solution was electrolytically reduced to the aquo U^{4+} ion using a conventional 3-electrode system at a potential of -0.22V (vs. SCE). The solution was subsequently electrochemically re-oxidized to the UO_2^{2+} ion at about 1.10V (vs. SCE). This resulted in a UO_2^{2+} solution that was 10% enriched in ^{17}O. The oxidation states were confirmed using UV-VIS-NIR spectroscopy to identify the U(IV) peak at 648nm (ε = 59 M^{-1} cm^{-1})[58] and the U(VI) peak at 414 nm (ε = 7.6 M^{-1} cm^{-1})[59] at each stage of the electrolysis. The $U^{17}O_2^{2+}$ was

then precipitated as the hydroxide between $4.5 \leq pH \leq 7$. The precipitate was isolated by centrifugation, and then washed 3 times with H_2O. A solution of ^{17}O labeled carbonate was made by combining 2.32 mL of 43% $H_2{}^{17}O$, 2.4 mL D_2O, and 0.28 mL of 10.7 M supra-pure (carbonate-free) NaOH to make a 0.6 M NaOH solution. This solution was placed in a PARR pressure vessel and charged with 5 atmospheres of CO_2 with stirring. The solution was allowed to equilibrate for 48 h, to produce 5 mL of 0.6 M ^{17}O-enriched $NaHCO_3$. The ^{17}O-enriched uranyl hydroxide precipitate was dissolved in 4.25 mL of the freshly-prepared ^{17}O-enriched $NaHCO_3$. The resulting slurry was mixed on a vortex mixer for several minutes, then placed in an ultrasonic bath for 10 min until all the solid had dissolved, and a clear yellow solution resulted. $NaClO_4 \cdot H_2O$ (0.598 g, 7.1 mmol) was added to make the ionic strength of solution 3.3 mol/kg. $1M$ $HClO_4$ and solid Na_2CO_3 were used to adjust the pH and obtain samples in the pH range from 6.0 $\leq pH \leq 9.7$. Samples were sealed in 5mm NMR tubes and pH values near a pH of 6 were stabilized by using CO_2 flushed NMR tubes.

4.7 Solution Preparations. ^{13}C - enriched solutions.

Single crystals of $UO_2(ClO_4)_2(H_2O)_6$ (1.739 g, 3.0 mmol) were dissolved in 2.0 mL D_2O. $Na_2{}^{13}CO_3$ (0.954 g, 8.9 mmol) and $NaClO_4(H_2O)$ (2.104 g, 25 mmol) were dissolved in 13 mL of D_2O in a 50 mL Oak Ridge centrifuge tube. The uranium solution was slowly added to this carbonate solution with stirring to make a solution which was 0.2 M in uranium, 0.6 M in sodium carbonate and 1.0 M in sodium perchlorate. $1M$ $HClO_4$ was used to adjust the pH of the solution to get the 5 samples with pH values ranging from pH of 9.04 to 5.97. Samples were sealed in standard 5mm NMR tubes, those at lower pH were sealed in tubes flushed with CO_2 to stabilize the pH. Another sample at $I_m = 2.5$ m was similarly prepared to make a solution which was 0.05 M in uranium, and 0.15 M in sodium carbonate, and 1.8 M in $NaClO_4$. $1M$ $HClO_4$ was used to adjust the pH of the solution to get the 17 samples with pH values ranging from pH of 9.0 to 5.7.

47

Samples were sealed in standard 5mm NMR tubes, those at lower pH were sealed in tubes flushed with CO_2 to stabilize the pH.

4.8   Synthesis of $(UO_2)(CO_3)_3[CN_3H_6]_4$ (1). To a solution of 0.504 g (1.0 mmol) of $UO_2 (NO_3)_2 \cdot 6 H_2O$ in 0.5 ml of distilled water was added dropwise to a solution of 0.541 g (3.0 mmol) of guanidine carbonate in 9.5 mL of distilled water with stirring. The resulting 10 mL of solution was 0.1 M in uranium and 0.3 M in carbonate, and a pH of 9.53. The solution was then sealed in a argon purged 20 mL glass scintillation vial, wrapped in parafilm, and stored at 0° C. After 24 hrs, large cubic crystals of a bright-yellow crystalline solid resulted. IR (KBr, Nujol, cm^{-1}) 3475 (vs, br), 1526 (s), 1343 (s), 1143 (m), 1054 (m), 892(s), 866 (m), 811 (w), 687 (m), 530 (m). Anal. Calcd. for $UO_{17}N_{12}C_7H_{24}$: C, 12.19; H, 3.50; N, 24.35. Found: C, 12.95; H, 3.22; N, 23.74.

4.9   Synthesis of $(UO_2)_3(CO_3)_6[CN_3H_6]_6$ (2). To a solution of 0.504 g (1.0 mmol) of $UO_2 (NO_3)_2 \cdot 6 H_2O$ in 0.5 ml of distilled water was added dropwise a solution of 0.541 g (3.0 mmol) of guanidine carbonate in 9.5 mL of distilled water with stirring. The resulting 10 mL of solution was 0.1 M in uranium and 0.3 M in carbonate. The pH of the uranyl carbonate solution was slowly adjusted using 1M HCl, and a stream of CO_2 was passed over the solution to stabilize at a final pH of 6.12. The solution was then sealed in a CO_2 purged 20 mL glass scintillation vial, wrapped in parafilm, and stored at 0° C. After 24 hrs, thin needle-like plates of a bright-yellow crystalline solid resulted. IR (KBr, Nujol, cm^{-1}) 3352 (vs, br), 1672 (s), 1519 (s), 1464 (s), 1378 (s), 1339 (s), 1141 (m), 1047 (m), 886(s), 731 (s), 535 (m). Anal. Calcd. for $U_3O_{24}N_{18}C_{12}H_{36}$: C, 9.42; H, 2.37; N, 16.47. Found: C, 10.21; H, 2.61; N, 19.00.

5.0   References

1.   Choppin, G. R.; Stout, B. E. "Actinide Behavior in Natural Waters" *Sci. Tot. Environ.* **1989**, *83*, 203.   NNA.94032.0276

2.   Choppin, G. R.; Allard, B. in *Handbook of the Chemistry and Physics of the Actinides*; Freeman, A. J., Keller, C., Eds.; Elsevier, Amsterdam, **1985**; Vol 3, Chapter 11. Readily available.

3.   Nash, K. L.; Cleveland, J. M.; Rees, T. F. "Speciation Patterns of Actinides in Natural Waters: a Laboratory Investigation" *J. Environ. Radioactivity* , **1988**, *7* , 131. NNA.940121.0176.

4.   Kim, J. I. "Chemical Behaviour of Transuranic Elements in Natural Aquatic Systems" in *Handbook of the Chemistry and Physics of the Actinides*; Freeman, A. J., Keller, C., Eds.; Elsevier, Amsterdam, **1986**; Vol 4, Chapter 8. HQS.880517.3116

5.   Hobart, D. E. "Actinides in the Environment" in *Proceedings of the Robert A. Welch Foundation Conference on Chemical Research XXXIV: Fifty Years with Transuranium Elements*, Chapter XIII, Houston, TX, October 22-24, **1990**, 379, and references therein. NNA.930405.0083

6.   Grenthe,I.; Lemire, R. J.; Muller, A. B.; Nguyen-Trung, C.; Wanner, H.; *Chemical Thermodynamics of Uranium*; OEDC-NEA: Paris, **1991**. NNA.900816.0013

7.   Christ, C. L.; Clark, J. R.; Evans, H. T., Jr. "Crystal Structure of Rutherfordine, UO_2CO_3" *Science*, **1955**, *121*, 472. NNA.940121.0177.

8.   Coda, A.; Della Giusta, A.; Tazzoli, V. "The Structure of Synthetic Andersonite, $Na_2Ca[UO_2(CO_3)_3] \cdot H_2O$ (x $\approx$ 5,6)" *Acta. Cryst.* **1981**, *B37*, 1496. NNA.931214.0048.

9.   Martell, A. E.; Motekaitis, R. J. *"Determination and Use of Stability Constants;"* VCH Publishers: New York, **1988**. Readily available.

10.   Blake, C. A.; Coleman, C. F.; Brown, K. B.; Hill, D. G.; Lowrie, R. S.; Schmitt, J. M. "Studies in the Carbonate - Uranium System" *J. Am. Chem. Soc.*, **1956**, *78*, 5978. HQS.880517.1958

11.   Paramonova, V. I.; Nikol'skii, B. P.; Nikolaeva, N. M. "Interaction of Uranyl in Nitrate Solutions" *Russ. J. Inorg. Chem.*, **1962**, *7*, 528. NNA.940323.0281.

12.   Sergeyeva, E. I.; Nikitin, A. A.; Khodakovsky, I. L.; Naumov, G. B."Experimental Investigation of Equilibria in the System UO_3-CO_2-H_2O in 25 - 200 °C Temperature Interval" *Geochim. Int.*, **1972**, *11*, 900. NNA.940121.0179.

13.   Almagro, V.; Garcia, F. S.; Sancho, "Estudio Polarografico Del Ion UO_2^{2+} en Medio Carbonato Sodio" *J. An. Quim.*, **1973**, *69*, 709. NNA.94032.0275.

14.   Cinnéide, S. O.; Scanlan, J. P.; Hynes, M. J., "Equilibria in Uranyl Carbonate Systems: I. The Overall Stability Constant of $UO_2(CO_3)_3^{4-}$" *J. Inorg. Nucl. Chem.* **1975**, *37*, 1013. NNA.940323.0271.

15.   Nikolaeva, N. M., "Solubility Product of UO_2CO_3 at Elevated Temperature" *Izv. Sib. Otd. Akad. Nauk SSSR*, **1976**, *6*, 30. NNA.940121.0180.

16.   Ciavatta, L.; Ferri, D.; Grimaldi, M.; Palombari, R.; Salvatore, F. "Dioxouranium(VI) Carbonate Complexes in Acid Solution" *J. Inorg. Nucl. Chem.* **1979**, *41*, 1175. NNA.931214.0047.

17.   Maya, L.; Begun, G. M. "A Raman Spectroscopic Study of Hydroxo and Carbonato Species of the Uranyl(VI) Ion" *J. Inorg. Nucl. Chem.* **1981**, *43*, 2827. NNA.940121.0181.

18.   Ferri, G.; Grenthe, I.; Salvatore, F. "Dioxouranium(VI) Carbonate Complexes in Neutral and Alkaline Solutions" *Acta Chem. Scand.* **1981**, *A35*, 165. NNA.940121.0182.

19.   Maya, L. "Hydrolysis and Carbonate Complexation of Dioxouranium(VI) in the Neutral-pH Range at 25 °C" *Inorg. Chem.* **1982**, *21*, 2895. NNA.940103.0069.

20.   Grenthe, I.; Ferri, D.; Salvatore, F.; Riccio, G. "Studies on Metal Carbonate Equilibria. Part 10. A Solubility Study of the Complex Formation in the Uranium(VI)-Water-Carbon Dioxide (g) System at 25 °C" *J. Chem. Soc. Dalton Trans.* **1984**, 2439. NNA930707.0050

21.   Grenthe, I.; Lagerman, B. "Studies on Metal Carbonate Equilibria. 22. A Coulometric Study of the Uranium(VI)-Carbonate System, the Composition of the Mixed Hydroxide Carbonate Species" *Acta Chem. Scand.* **1991**, *45*, 122. NNA.940323.0272.

22.   Ullman, W. J.; Schreiner, F. "Calorimetric Determination of the Enthalpies of the Carbonate Complexes of U(VI), Np(VI), and Pu(VI) in Aqueous Solution at 25 °C" *Radiochim. Acta.* **1988**, *43*, 37. NNA.940103.0068.

23.   Ciavatta, L.; Ferri, D.; Grenthe, I.; Salvatore, F. "The First Acidification Step of the Tris(carbonato)dioxouranate(VI) Ion, $UO_2(CO_3)_4^-$" *Inorg. Chem.* **1981**, *20*, 463. NNA.940323.0279.

24.   Åberg, M.; Ferri, D.; Glaser, J.; Grenthe, I. "Studies of Metal Carbonate Equilibria. 8. Structure of the Hexakis(carbonato)tris[dioxourante(VI)] Ion in Aqueous Solution. An X-ray Diffraction and ^{13}C NMR Study" *Inorg. Chem.* **1983**, *22*, 3981. NNA930707.0051

25.   B. E. Stout, G. R. Choppin, and J. C. Sullivan, "The Chemistry of Uranium(VI), Neptunium(VI), and Plutonium(VI) in Aqueous Carbonate Soluitions," in *Transuranium Elements, A Half Century*, L. R. Morss, and J. Fuger, Eds. American Chemical Society, Washington D.C.,**1992**, 225. NNA.930707.0053

26.   Brücher, E.; Glaser, J.; Toth, I."Carbonate Exchange for the Complex $UO_2(CO_3)_3^{4-}$ in Aqueous Solution As Studied by ^{13}C NMR Spectroscopy" *Inorg. Chem.*, **30**, 2239 (1991). NNA.930707.0052

27.   Strom, E. T.; Woessner, D. E.; Smith, W. B. "^{13}C NMR Spectra of the Uranyl Tricarbonate-Bicarbonate System" *J. Am. Chem. Soc.*,**1981**, *103* , 1255. NNA.940124.0040.

28.   Graziani, R.; Bombieri, G.; Forsellini, E. "Crystal Structure of Tetra-ammonium Uranyl Tricarbonate" *J. Chem. Soc. Dalton, Trans.* **1972**, *19*, 2059. NNA.940121.0183.

29. Mereiter, K. "Structure of Caesium Tricarbonatodioxouranate(VI) Hexahydrate" *Acta Crystallogr.* **1988**, *C44*, 1175. NNA.940121.0184.

30. Simakin, G. A. "Real Oxidation Potentials of the Couples AmO_2^{2+} - AmO_2^+, NpO_2^{2+} - NpO_2^+ in Solutions of Potassium and Sodium Carbonates" *Radiokhimiya,* **1977**, *19* , 424. NNA.940121.0185.

31. Maya, L. "Carbonate Complexation of Dioxoneptunium(VI) at 25 °C: Its Effect on the Np(V)/Np(VI) Potential" *Inorg. Chem.* **1984**, *23*, 3926. NNA.940121.0186.

32. Marquart, R.; Hoffmann, G.; Weigel, F. "Preparation and Properties of Complex Carbonates of Hexavalent Actinides" *J. Less-Common Met.*, **1983**, *91*, 119. NNA.940121.0187.

33. Madic, C.; Hobart, D. E.; Begun, G. M. "Raman Spectrometric Studies of Actinide(V) and -(VI) Complexes in Aqueous Sodium Carbonate Solution and of Solid Sodium Actinide(V) Cjarbonate Compounds" *Inorg. Chem.* **1983**, *22*, 1494. NNA.940103.0067.

34. Basile, L. J.; Ferraro, J. R.; Mitchell, M. L.; Sullivan, J. C. "The Raman Scattering of Actinide(VI) ions in Carbonate Media" *Appl. Spectroscopy.* **1978**, *32*, 535. NNA.940323.0277.

35. Nguyen-Trung, C.; Begun, G. M.; Palmer, D. A. "Aqueous Uranium Complexes. 2. Raman Spectroscopic Study of the Complex Formation of the Dioxouranium(VI) Ion with a Variety of Inorganic and Organic Ligands" *Inorg. Chem.* **1992**, *31*, 5280. NNA.940121.0188.

36. Grenthe, I.; Riglet, C.; Vitorge, P., "Studies of Metal-Carbonate Complexes. 14. Composition and Equilibria of Trinuclear Neptunium(VI)- and Plutonium(VI)-Carbonate Complexes" *Inorg. Chem.*, **1986**, *25*, 1679. NNA.940121.0189.

37. Ferri, D.; Glaser, J.; Grenthe, I."Confirmation of the Structure of $(UO_2)_3(CO_3)_6^{6-}$ by ^{17}O NMR" *Inorg. Chim. Acta*, **1988**, *148*, 133. NNA.940124.0037.

38. Friebolin, H., "Basic One- and Two-Dimensional NMR Spectroscopy", VCH Publishers, New York, N.Y. **1991**. Readily available.

39. Boykin, D. W. "^{17}O NMR Spectroscopy in Organic Chemistsry", CRC Press, Boca Raton, **1991**. Readily available.

40. Klemperer, W. G. "^{17}O-NMR Spectroscopy as a Structural Probe" *Angew Chem. Int. Ed., Engl.* **1978**, *17*, 246. NNA.940323.0280.

41. Gordon, G.; Taube, H. "The Uranium(V)-Catalysed Exchange Reaction Between Uranyl Ion and Water in Perchloric Acid Solution" *J. Inorg. Nucl. Chem.*, **1961**, *16*, 272. NNA.940121.0190.

42. Rabideau, S. W. "Oxygen-17 Nuclear Magnetic Resonance in the Uranyl Ion"*J. Phys. Chem.*, **1967**, *71*, 2747. NNA.940202.0092.

43. Murman, R. K.; Sullivan, J. C. "The Formation of a Neptunium(V)-Rhodium(III) Complex. Kinetics and Equilibria in Acidic Solutions" *Inorg. Chem.* **1967**, *6*, 892. NNA.940121.0190.

44. Newton, T. W., Hobart, D. E. and Palmer, P. D. "The Preparation and Stability of Pure Oxidation States of Neptunium, Plutonium, and Americium," *Los Alamos National Laboratory Report No. LA-UR-86-967*, **1986**, Los Alamos, New Mexico. NNA.930406.0025

45. Kritchevsky, E. S.; Hindman, J. C. "The Potentials of the Uranium Three-Four and Five-Six Couples in Perchloric and Hydrochloric Acids" *J. Am. Chem. Soc.*, **1949**, *71*, 2096. NNA.940121.0192.

46. Figgis, B. N.; Kidd, R. G.; Nyholm, R. S. "Oxygen-17 Nuclear Magnetic Resonance of Inorganic Compounds" *Proc. Royal Soc. A.*, **1962**, *A269*, 469. NNA.940121.0193.

47. Jung, W-S.; Ikeda, Y.; Tomiyasu, H.; Fukutomi, H. "Oxygen Isotope Shifts in ^{17}O NMR Spectra of the Uranyl Ion" *Bull. Chem. Soc. Japan*, **1984**, *57*, 2317. NNA.940121.0194.

48. Jung, W-S.; Tomiyasu, H.; Fukutomi, H. "Oxygen-17 NMR Study of the Uranyl Ion. II. Correlation between ^{17}O NMR Chemical Shifts and Wavelengths of UV-Visible Absorption Bands of Uranyl Complexes" *Bull Chem. Soc. Jpn*, **1985**, *58*, 938. NNA.940323.0278.

49. Baes, C. F. and Mesmer, R. E. "The Hydrolysis of Cations", J. Wiley and Sons, N. Y. **1976**. HQS.880517.1945

50. Robinson, R. A.; Stokes, R. H. "Electrolyte Solutions", Butterworths Scientific Publications, London, **1955**. Readily available

51. Westcott, C. C. "pH Measurements", Academic Press, NY, **1978**. Readily available.

52. Linder, P. W.; Torrington, R. G.; Williams, D. R. "Analysis Using Glass Electrodes", Open University Press, Milton Keynes, **1984**. Readily available.

53. Feldman, I. "Use and Abuse of pH Measurements" *Anal. Chem.* **1956**, *28*, 1859. NNA.940323.0279.

54. Glassley, W. E. "Reference Waste Package Enevironment Report", UCRL-53726, Lawrence Livermore National Laboratory, **1986**. NNA.920506.0035

55. U.S. Department of Energy, **1988**. "Site Characterization Plan, Groundwater chemistry, Yucca Mountain Site, Nevada Research and Development Area, Nevada," DOE/RW-0199, vol II, Part A, Chapt 4, Section 4.1.2. Nuclear Waste Policy Act (Section 113), Office of Civilian Radioactive Waste Management, Washington, DC. HQS.880517.2987

56. U.S. Department of Energy, **1988**. "Site Characterization Plan, Reference Groundwater Composition, Yucca Mountain Site, Nevada Research and Development Area, Nevada," DOE/RW-0199, vol II, Part A, Chapt 4, Section 4.1.2.10 Nuclear Waste Policy Act (Section 113), Office of Civilian Radioactive Waste Management, Washington, DC. HQS.880517.2987

57.   Hobart, D. E.; Samhoun, K.; Peterson, J. R. "Spectroelectrochemical Studies of the Actinides: Stabilizatio of Americium(IV) in Aqueous Carbonate Solution" *Radiochim. Acta.* **1982**, *31*, 139.   NNA.940103.0070.

58.   K.A. Kraus and F. Nelson, "Hydrolytic Behavior of Metal Ions.   I.   The Acid Constants of Uranium(IV) and Plutonium(IV)" *J. Amer. Chem. Soc.*, **1950**, *72*, 3901. NNA.940121.0195.

59.   R. Sjoblom and J. C. Hindman, "Spectrophotometry of Neptunium in Perchloric Acid Solutions" *J. Amer. Chem. Soc.*, **1951**, *73*, 1744.   NNA.940323.0273.

6.0 Quality Assurance Documentation

Data in this paper is documented in laboratory notebooks TWS-INC-01-93-12, TWS-INC-11-11-88-9, and TWS-INC-12-92-04. Because some of the software used for data collection / manipulation has not been officially sanctioned by the Yucca Mt. Site Characterization Project QA program, the data presented here may be non-quality affecting for the project. Preassigned accession number NNA.931021.0073.